Title

Heterogeneous transgene expression in the retinas of the TH-RFP, TH-Cre, TH-BAC-Cre and DAT-Cre mouse lines

Authors

Vuong, HE
de Sevilla Müller, L Pérez
Hardi, CN
et al.

Publication Date

2015-10-01

DOI

10.1016/j.neuroscience.2015.08.060

Peer reviewed

HHS Public Access

Author manuscript

Neuroscience. Author manuscript; available in PMC 2016 October 29.

Published in final edited form as:

Neuroscience. 2015 October 29; 307: 319–337. doi:10.1016/j.neuroscience.2015.08.060.

Heterogeneous transgene expression in the retinas of the TH-RFP, TH-Cre, TH-BAC-Cre and DAT-Cre mouse lines

Helen E. Vuong[1,2,3], **Luis Pérez de Sevilla Müller**[2], **Claudia N. Hardi**[4], **Douglas G. McMahon**[6], and **Nicholas C. Brecha**[1,2,3,5,7]

[1]Molecular, Cellular, and Integrative Physiology Program, David Geffen School of Medicine at UCLA, Los Angeles, CA 90095

[2]Department of Neurobiology, David Geffen School of Medicine at UCLA, Los Angeles, CA 90095

[3]Jules Stein Eye Institute, David Geffen School of Medicine at UCLA, Los Angeles, CA 90095

[4]Department of Psychology, David Geffen School of Medicine at UCLA, Los Angeles, CA 90095

[5]CURE-Digestive Diseases Research Center, David Geffen School of Medicine at UCLA, Los Angeles, CA 90095

[6]Department of Biological Sciences, Vanderbilt University, Nashville, TN 37235

[7]Veterans Administration Greater Los Angeles Healthcare System, Los Angeles, CA 90073

Abstract

Transgenic mouse lines are essential tools for understanding the connectivity, physiology and function of neuronal circuits, including those in the retina. This report compares transgene expression in the retina of a tyrosine hydroxylase (TH)-red fluorescent protein (RFP) line with three catecholamine-related Cre recombinase lines [TH-bacterial artificial chromosome (BAC)-, TH-, and dopamine transporter (DAT)-Cre] that were crossed with a ROSA26-tdTomato reporter line. Retinas were evaluated and immunostained with commonly used antibodies including those directed to TH, GABA and glycine to characterize the RFP or tdTomato fluorescent-labeled amacrine cells, and an antibody directed to RNA-binding protein with multiple splicing to identify ganglion cells. In TH-RFP retinas, types 1 and 2 dopamine (DA) amacrine cells were identified by their characteristic cellular morphology and type 1 DA cells by their expression of TH immunoreactivity. In the TH-BAC-, TH-, and DAT-tdTomato retinas, less than 1%, ~6%, and 0%, respectively, of the fluorescent cells were the expected type 1 DA amacrine cells. Instead, in the TH-BAC-tdTomato retinas, fluorescently labeled AII amacrine cells were predominant, with some medium somal diameter ganglion cells. In TH-tdTomato retinas, fluorescence was in multiple neurochemical amacrine cell types, including four types of polyaxonal amacrine cells. In DAT-tdTomato retinas, fluorescence was in GABA immunoreactive amacrine cells, including two types

Corresponding author: Nicholas C. Brecha, PhD., Department of Neurobiology, David Geffen School of Medicine at UCLA, University of California at Los Angeles, 10833 Le Conte Ave., Los Angeles, California 90095-1763, nbrecha@ucla.edu, Phone: 310-825-6758, Fax: 310-825-2224.

of bistratified and two types of monostratified amacrine cells. Although each of the Cre lines were generated with the intent to specifically label DA cells, our findings show a cellular diversity in Cre expression in the adult retina and indicate the importance of careful characterization of transgene labeling patterns. These mouse lines with their distinctive cellular labeling patterns will be useful tools for future studies of retinal function and visual processing.

Keywords

Transgenic; Cre-lox-system; GABA; glycine; dopamine; amacrine cells

Introduction

Transgenic mouse models are one of the major tools currently used for investigations of the intricate anatomical, biophysical and functional properties of neuronal cell populations and their networks. For instance, studies using mouse models have contributed to the identification and manipulation of the connectivity, interactions and activity of neurons within a network, which has advanced our understanding of their functional role in neuronal processing in multiple structures, including the retina, cortex, hippocampus, olfactory bulb and cerebellum (Ramirez et al., 2013, Hammen et al., 2014, Pohlkamp et al., 2014, Robinson et al., 2014, Sternson and Roth, 2014, Zhu et al., 2014a, Zhu and Roth, 2014). The use of transgenic mouse models has been especially powerful for studies of intrinsic retinal circuitry and function, including those of amacrine and ganglion cell subtypes, as well as the understanding of the functional connectivity of retinal ganglion cells with central visual nuclei (Kim et al., 2010, Kay et al., 2011a, Rivlin-Etzion et al., 2011, Yamagata and Sanes, 2012, Zhang et al., 2012, Dhande et al., 2013, Farrow et al., 2013, Yonehara et al., 2013, Vlasits et al., 2014, Zhu et al., 2014b).

Amacrine cells are classified based on their general morphology, including somal size, the stratification pattern of their processes in the inner plexiform layer (IPL), and their neurochemical expression (Boycott and Wässle, 1974, Brecha et al., 1979, Karten and Brecha, 1980, Kolb et al., 1981, Vaughn et al., 1981, Masland, 1988, Casini and Brecha, 1991). Based on these criteria, 30 to 40 different amacrine cell types have been identified in the mammalian retina (Kolb and Nelson, 1981, Xin and Bloomfield, 1997, MacNeil and Masland, 1998, MacNeil et al., 1999, Masland, 2001, Badea and Nathans, 2004). Furthermore, the microcircuits these cells form are likely to mediate different functions in visual processing within the retina (Masland, 2001, Wässle, 2004).

One well-studied wide-field amacrine cell type is the tyrosine hydroxylase (TH) or dopamine (DA) amacrine cell, which is also known as a type 1 DA amacrine cell. This amacrine cell synthesizes and releases dopamine, in addition to the inhibitory neurotransmitter GABA (Wulle and Wagner, 1990, Hirasawa et al., 2009, Contini et al., 2010, Hirasawa et al., 2012). The morphology of type 1 DA amacrine cells have been thoroughly characterized in retinas of multiple species, including amphibians, rodents, lagomorphs, felines and primates using antibodies against TH, the rate-limiting enzyme for the synthesis of dopamine (Brecha et al., 1984, Versaux-Botteri et al., 1984, Oyster et al.,

1985, Mariani and Hokoç, 1988, Nguyen-Legros, 1988, Dacey, 1990, Tauchi et al., 1990, Zhu and Straznicky, 1990). Physiological studies indicate multiple retinal functions for dopamine, including a role in light/dark adaptation of retinal circuits and serving as the output of the retinal circadian clock. Moreover, low levels of dopamine are often concomitant with retinal disease including diabetic retinopathy (Teakle et al., 1993, Witkovsky, 2004, Aung et al., 2014).

The identification of type 1 DA amacrine cells in transgenic lines have been of great value in determining the circuits they participate in within the inner retina. For example, transgenic labeling of type 1 DA amacrine cells have aided in defining the connectivity between these cells and AII and GABA-containing amacrine cells, ON-cone bipolar cells, and melanopsin-containing ganglion cells (Gustincich et al., 1997, Feigenspan et al., 2000, Zhang et al., 2007, Contini et al., 2010, Van Hook et al., 2012, Zhang et al., 2012, Newkirk et al., 2013). Other studies that used isolated type 1 DA amacrine cells, labeled by human placental alkaline phosphatase (hPLAP), report these cells have transient A-type K^+, Ca^{2+} and TTX-sensitive Na^+ currents, and rhythmic spontaneous action potentials (Feigenspan et al., 1998, Xiao et al., 2004). More recently, type 1 DA amacrine cells identified by green fluorescent protein (GFP) in retinal whole mounts of a dopamine receptor 2 transgenic mouse line were used to characterize their resting spontaneous spike properties and light responses (Newkirk et al., 2013).

Despite many advances in understanding type 1 DA amacrine cell function, their functional influence on other cells in the retinal network has not been completely established. Studies addressing this topic would be greatly facilitated by using a mutant mouse line with Cre recombinase activity exclusively in type 1 DA amacrine cells to genetically manipulate these cells. In this study, we have evaluated three catecholamine-related transgenic mouse lines expressing Cre, and compared them to a previously published TH-RFP mouse line with DA amacrine cells expressing red fluorescent protein (RFP) (Zhang et al., 2004). Cre expression under the control of TH or dopamine transporter (DAT) regulatory elements is expected to provide specific labeling of the type 1 DA amacrine cells in the retina, as in the rest of the central nervous system (Gelman et al., 2003, Lindeberg et al., 2004, Zhuang et al., 2005, Bäckman et al., 2006). However, our studies of the cellular localization of Cre reporter expression in the retinas of these mouse lines show that there is a surprisingly small percentage or a lack of type 1 DA amacrine cells labeled in these retinas. In contrast, these retinas contained ectopic yet reliably identifiable Cre-dependent fluorescently labeled cell types in the inner retina, including AII, polyaxonal amacrine cells, monostratified and bistratified amacrine cells, displaced amacrine cells, and a few ganglion cells. These Cre-expressing mouse lines will be of value to other investigations of the aforementioned amacrine cells.

Materials and Methods

Animal care and all experiments were carried out in accordance with the guidelines for the welfare of experimental animals issued by the U.S. Public Health Service Policy on Human Care and Use of Laboratory Animals and the University of California Los Angeles (UCLA) Animal Research Committee.

Mouse lines

Tyrosine hydroxylase-Cre recombinase (TH-Cre) (B6.Cg-Tg (TH-Cre)1Tmd/J; #008601) and dopamine transporter-Cre (DAT-Cre) (B6.SJL-Slc6a3$^{tm1.1(cre)}$Bkmn/J; #006660) transgenic mouse lines were obtained from The Jackson Laboratory (Bar Harbor, ME). The TH-bacterial artificial chromosome-Cre (TH-BAC Cre) (Tg (TH-Cre) fI172Gsat/Mmucd; #029177-UCD) transgenic mouse line was obtained from the Mutant Mouse Regional Resource Centers (MMRRC at University of California, Davis, California). The Cre-dependent tdTomato (B6.Cg-Gt (ROSA)26Sor$^{tm14(CAG-tdTomato)Hze}$/J; #007908) reporter line was obtained from The Jackson Laboratory. The TH-red fluorescent protein (TH-RFP) mouse line was developed by Dr. Douglas G. McMahon and bred at UCLA for these studies (Zhang et al., 2004).

Mouse lines (DAT-tdTomato, TH-tdTomato, and TH-BAC-tdTomato) were generated by crossing the Cre-recombinase transgenic mouse lines: TH-Cre (Savitt et al., 2005), DAT-Cre (Bäckman et al., 2006) and TH-BAC Cre (Gong et al., 2007) to a tdTomato reporter line (Ai14) (Madisen et al., 2010). Breeding was carried out in the UCLA Division of Laboratory Animal Medicine facility, and offspring were genotyped to check for Cre and reporter expression. Primers used for detecting Cre were oIMR1084 (5′-GCG GTC TGG CAG TAA AAA CTA TC-3′) and oIMR1085 (5′-GTG AAA CAG CAT TGC TGT CAC TT-3′). A predicted band at ~100 bp indicated the presence of the Cre transgene. Detection of tdTomato required two primer sets: 1) oIMR9020 (5′-AAG GGA GCT GCA GTG GAG TA-3′) and oIMR9021 (5′-CCG AAA ATC TGT GGG AAG TC-3′) for wild-type forward and reverse primers, and 2) oIMR9103 (5′GGC ATT AAA GCA GCG TAT CC-3′) and oIMR9105 (5′-CTG TTC CTG TAC GGC ATG G-3′) for the presence of tdTomato. A predicted band at 196 bp indicated the transgene for tdTomato, and heterozygote mice had predicted bands at 196 and 297 bp. The TH-RFP transgenic mouse line contained a TH-RFP transgene consisting of a 4.5 kb fragment of the rat tyrosine hydroxylase promoter ligated to DsRed2-1 (Zhang et al., 2004). Primers used for detecting RFP were 5′-GCA CCT TGA AGC GCA TGA A-3′ and 5′-CAC TTT GTT ACA TGG GCT GGG-3′. A predicted band at ~590 bp indicated the presence of the transgene.

Tissue preparation

Male and female adult mice (4–6 weeks old) were deeply anesthetized using 1–3% isofluorane (IsoFlo, Abbott Laboratories, North Chicago, IL) and killed by decapitation or cervical dislocation. Eyes were enucleated, and the cornea and lens were removed.

Vertical retinal sections—Eyecups were immersion fixed in 4% (w/v) paraformaldehyde (PFA) in 0.1 M phosphate buffer (PB), pH 7.4 for 15–60 minutes. Eyecups were subsequently washed in 0.1 M PB for 30 minutes and stored in 30% sucrose overnight at 4°C, and then embedded in optimal cutting temperature medium (Sakura Finetek Inc., Torrance, CA) and sectioned vertically at 12 μm. Retinal sections were placed onto gelatin-coated slides and stored at −20°C until used for immunohistochemistry.

Whole-mount retinal preparation—The retinas were removed from the eyecups, and four small incisions were made to lay the retina flat. Retinas were mounted, ganglion cell

layer (GCL) up, onto nitrocellulose membrane filters (cat #HABP04700; Millipore Corporation, Billerica, MA), and fixed for 30–60 minutes in 4% PFA in 0.1M PB at room temperature. Whole-mounted retinas were then processed for immunohistochemistry.

Immunohistochemistry

Vertical retinal sections—Retinal sections were processed for immunohistochemical labeling using an indirect immunofluorescence method (Hirano et al., 2005). Frozen retinal sections were thawed for 10 minutes at 37°C on a warming plate, then washed three times for 10 minutes with 0.1 M PB (pH 7.4). Sections were then incubated in a blocking solution of 10% normal goat serum (NGS), 1% bovine serum albumin (BSA) and 0.5% Triton X-100 in 0.1 M PB for 1 hour at room temperature. Following removal of the blocking solution, the primary antibody solution was immediately added to the sections and incubated for 12–16 hours at 4°C. Primary antibody solution contained 3% NGS, 1% BSA, 0.05% sodium azide and 0.5% Triton X-100 in 0.1 M PB. Retinal sections were then washed three times for 10 minutes in 0.1 M PB. The sections were then incubated in their corresponding secondary antibodies goat anti-rabbit, -rat or -mouse conjugated to Alexa 568 or 488 (1:1000; Invitrogen, Grand Island, NY) for two hours at room temperature. The secondary antibody was removed and sections were washed three times in 0.1 M PB for 10 minutes per wash. Sections were air-dried and mounted using Aqua Poly/Mount (Polysciences, Warrington, PA). To control for nonspecific binding of the secondary antibody, the primary antibodies were omitted in the single-labeling studies.

Whole-mounted retina—Whole-mounted retinas were processed for immunohistochemical labeling with a protocol similar to that used for vertical sections. Whole-mounted retinas were fixed, washed in 0.1 M PB and then incubated in blocking solution overnight at 4°C. The retinas were then transferred to primary antibody solution and incubated for 5 days at 4°C. Retinas were washed in 0.1 M PB for 3 times for 20 minutes each time, and then incubated in secondary antibodies for 2 days at 4°C. Following removal from secondary antibody solution, retinas were washed three times in 0.1 M PB for 20 minutes for each wash. Similar to the retinal sections, whole-mounted retinas were briefly air-dried and mounted using Aqua Poly/Mount.

Antibodies

Retinal sections and whole mounts were processed with the following primary antibodies and dilutions: mouse monoclonal antibody against tyrosine hydroxylase (TH) (1:2000; MAB5280 clone 2/40/15; Millipore), mouse polyclonal antibody against calretinin (1:2000; 010399 clone 6B3; Swant, Bellinzona, Switzerland), rabbit polyclonal antibody against GABA [1:2000 (transverse sections) and 1:500 (whole mount); A2052; Sigma-Aldrich, St Louis, MO, USA], rat polyclonal antibody against glycine [1:3000 (transverse sections) and 1:1000 (whole mount); IG1002; ImmunoSolution, Everton Park, Queensland, Australia], goat polyclonal against choline acetyltransferase (ChAT) (1:250; No. AB144P; EMD Millipore), and guinea pig polyclonal antibody against RNA-binding protein with multiple splicing (RBPMS; 1:20000; (Rodriguez et al., 2014)). The antibodies used in this study are listed in Table 1.

Confocal image acquisition

The immunostaining images were acquired with a Zeiss 510 Meta or 710 confocal laser scanning microscope (LSM, Carl Zeiss, Thornwood, NY) equipped with 488, 543, and 633 nm laser lines. Confocal scans were captured using a Plan Neofluar 25X 0.8 NA corrected water objective and a C-Apochromat 40X 1.2 NA corrected water objective. Projections of three images (1024 × 1024 pixels or 2048 × 2048 pixels) with a total of 0.9–1.0 μm thickness (z-axis step between 0.3–0.5 μm) were collected and adjusted for brightness and contrast in Adobe Photoshop CS2 v.9.02 (Adobe Systems, San Jose, CA).

Quantification of somal number, somal size, and field size

Digital images for cell counting were collected at 0.5 mm intervals from the optic nerve head to the peripheral retina in the superior, inferior, temporal and nasal retinal quadrants. Four retinal fields (425 × 425 μm^2) per quadrant were collected for each retina using a Plan Apochromat 20X/0.8 na corrected air objective with a 0.7–1.0 magnification factor or a Plan Apochromat 40X/1.2 na corrected water objective. Cells were manually counted from the digital images using cell counter in ImageJ (http://rsb.info.nih.gov/ij/index.html) to determine cell number and density (cells/mm^2).

Somal diameters and dendritic field sizes were measured from whole mounted retinas using Zeiss LSM image browser 510 proprietary software (version 3.2; Carl Zeiss). Diameters were calculated as the longest distance between any two points on an object's perimeter, or the maximum caliper. Field size measurements were made for five cells in each quadrant of a retina. These values were then averaged to determine average field size. Values reported are average ± standard deviation.

To characterize the cells expressing the transgenic reporter, whole-mounted retinal preparations of the TH-RFP, and the DAT-, TH-BAC-, and TH-tdTomato retinas were immunostained using multiple antibodies (Table 1), imaged and analyzed for co-expression. To determine the percent of co-localization, the number of RFP or tdTomato fluorescent cells and the number of immunoreactive cells that showed co-labeling were counted. Counts were made from 2–4 retinas from 2–4 different animals from each mouse line, and 16 retinal fields per retina.

Intracellular injections

Intracellular injections were performed as described previously (Pérez de Sevilla Müller et al., 2007, Müller et al., 2010a, Müller et al., 2010b). tdTomato-expressing cells were visualized with a Zeiss 40X water-immersion objective. Borosilicate glass electrodes (#60200; A-M Systems; Sequim, WA) were pulled and filled at their tips with 0.5% Lucifer Yellow (Sigma-Aldrich) 4% N-(2-aminoethyl)-biotinamide hydrochloride (Neurobiotin; Vector Laboratories, Burlingame, CA), and back-filled with 0.1 M Tris buffer, pH 7.4. Under visual guidance provided by the tdTomato fluorescence, cells were targeted for injection. First, Lucifer Yellow was iontophoresed (−1 nA) into the labeled cells and when its morphology could be visualized, the polarity of the current was reversed (+1 nA) and Neurobiotin was injected for 3 minutes. After the final injection, the retina was kept in the bath solution for at least 30 minutes to allow diffusion of the Neurobiotin. The retinas were

fixed in 4% PFA for 10 minutes. Neurobiotin was visualized by incubating injected retinas overnight at 4°C with streptavidin–FITC (1:500; Jackson ImmunoResearch, West Grove, PA) in 0.1 M PB containing 0.3% Triton X-100 (Sigma-Aldrich). Retinas were washed in PB 3 times for a total of 30 minutes and mounted in Vectashield (Vector Laboratories).

Results

General cellular labeling patterns in the TH-RFP, TH-BAC-tdTomato, TH-tdTomato, and DAT-tdTomato retinas

TH-RFP—As reported previously, TH-RFP retinas express RFP in sparsely distributed somata located in the proximal inner nuclear layer (INL) with numerous processes that ramify in the OFF layer of the IPL (Fig. 1A) (Zhang et al., 2004). A few varicose processes also ramified in the middle of the IPL (not shown) and in the outer plexiform layer (OPL) (Fig. 1A, arrow). There was a lower level of RFP expression in small caliber processes (Fig. 1A, arrowheads) and small somal diameter amacrine cells (not shown). Somal diameter and dendritic field size, as well as the cell's morphology were analyzed in whole-mount retinas. The average diameter of the large RFP fluorescent somata was 12.43 ± 2.33 μm (n=178 cells; 4 retinas; Table 2) and their average dendritic field size was about 850 μm (n=8 cells; 3 retinas) (Zhang et al., 2004). The morphology and distribution of the large RFP fluorescent cells in TH-RFP retinas are consistent with earlier descriptions of type 1 DA amacrine cells in the mouse retina (Fig. 2A) (Ballesta et al., 1984, Versaux-Botteri et al., 1984, Voigt and Wässle, 1987, Nguyen-Legros, 1988, Wulle and Schnitzer, 1989, Wulle and Wagner, 1990, Gustincich et al., 1997). The density of the type 1 DA amacrine cells was uniform throughout the retina with an average of 37 ± 17 cells/mm^2 (n=3 retinas; Table 2). TH-RFP retinas also contained another amacrine cell type (Fig. 2A, arrow) (Zhang et al., 2004). These cells had a lower level of fluorescence and a somal diameter of 9.89 ± 1.24 μm (n=136 cells; 2 retinas; Table 2). Their average density was 181 ± 54 cells/mm^2 (n= 2 retinas; Table 2). These observations are also consistent with an earlier report of type 2 DA amacrine cells in the TH-RFP retinas (Zhang et al., 2004).

TH-BAC-tdTomato—The TH-BAC-tdTomato retinas contained multiple small and medium diameter fluorescent cells that differed based on 1) their somal location in the proximal INL and GCL, and 2) the morphology and sparse distribution of their processes in multiple strata of the IPL (Fig. 1B and 2B). The most prominent type was a narrow-field amacrine cell in the proximal INL with processes that formed lobular processes in the OFF sublamina, and varicose arborizations in the ON sublamina of the IPL (Fig. 1B, arrowhead). These cells had a small somal diameter that measured 6.48 ± 1.04 μm, (n=300 cells; 4 retinas; Table 2). The morphological features of this amacrine cell type are similar to descriptions of AII amacrine cells (Casini et al., 1995, Wässle et al., 1995, Massey and Mills, 1999, Wässle et al., 2009, Pang et al., 2012). A group of medium diameter cells (9.10 ± 0.57 μm; n=71 cells; 4 retinas; Table 2) was also in the INL. In the GCL, there were a few, medium somal diameter ganglion cells (10.98 ± 2.24 μm, n=719 cells; 3 retinas; Table 2) with axonal processes in the nerve fiber layer (NFL) (Fig. 1B, arrows and 2B arrowheads to ganglion cell somata and their axons), and small diameter (6.86 ± 1.06 μm; n=139 cells; 2

retinas; Table 2) putative displaced amacrine cells based on the lack of an axonal process. The different cell types did not show regional differences in their density.

TH-tdTomato—The TH-tdTomato retinas also had multiple fluorescent cell types in the INL and GCL based on the stratification patterns of their processes in the IPL. Their processes mainly arborized in the OFF and ON-OFF sublaminae, and few processes arborized in the ON sublamina of the IPL (Fig. 1C and 2C). Fluorescent somata in the INL were found distal (arrowhead) and proximal (arrow) to the IPL (Fig. 1C). In the INL, cells were grouped into small (6.76 ± 0.99 μm; n=236 cells; 2 retinas; Table 2) and medium (10.11 ± 1.49 μm; n=84 cells; 2 retinas; Table 2) somal diameters. In the GCL, there were also two somal diameter groups, that measured 7.25 ± 1.02 μm and 10.34 ± 1.40 μm (n=36 and n=44 cells, respectively; 2 retinas; Table 2). The different sized cells in the INL and GCL had a similar density in all retinal regions. Medium diameter cells in both the INL and GCL had thick lateral processes (Fig. 2C) that extended over 500 μm in diameter (n=10 cells; 2 retinas). These cells were wide-field amacrine cells located in the INL or displaced into the GCL (Fig. 2C) (MacNeil and Masland, 1998, Völgyi et al., 2001, Völgyi et al., 2009).

DAT-tdTomato—In vertical sections of DAT-tdTomato retinas, there were numerous somata in the proximal INL (Fig. 1D) and GCL (Fig. 2D). Their processes were localized in a narrow band in the OFF sublamina proximal to the INL, and broadly in the ON sublamina of the IPL (Fig. 1D), suggesting multiple types of labeled cells in this line. Some of these cells in the INL had robust tdTomato-containing processes that extended into the ON sublamina of the IPL (Fig. 1D, arrows). The average somal diameter of the labeled cells in the INL was 8.97 ± 1.06 (n=42 cells) and GCL was 9.08 ± 1.61 (n=159 cells; 3 retinas; Table 2). The tdTomato cells were spread evenly across the retina, and there were no regional differences in density (646 ± 160 cells/mm^2 of retina; n=3 retinas; Table 2). Comparison of the tdTomato fluorescent somata counts in the GCL versus INL revealed fewer cells in the GCL (~13%) compared to the INL (~87%) (Fig. 2D).

Characterization of the fluorescent cells in the transgenic retinas using specific amacrine and ganglion cell immunohistochemical markers

TH-RFP retina—Previous studies have established that type 1 DA amacrine cells form a population of wide-field amacrine cells that robustly express TH-immunoreactivity in their somata and processes that mainly ramify in stratum 1 of the IPL in the mouse retina (Ballesta et al., 1984, Versaux-Botteri et al., 1984, Wulle and Wagner, 1990, Gustincich et al., 1997, Witkovsky, 2004). In the TH-RFP retinas, large diameter fluorescent amacrine cells in the INL and their processes contained TH immunoreactivity (Fig. 3A). TH immunostaining in finer caliber processes was more prominent compared to RFP fluorescence (Fig. 3A, arrowheads). All large diameter RFP fluorescent somata contained TH immunoreactivity and conversely all TH immunoreactive somata contained RFP fluorescence (Table 3) in all retinal regions of whole-mount preparations. Consistent with previous studies, the small diameter and weakly fluorescent somata did not contain TH immunoreactivity (not shown) (Gustincich et al., 1997, Zhang et al., 2004, Knop et al., 2011).

To aid in determining the level of stratification of the RFP fluorescent processes, we used a calretinin antibody, which labels amacrine cells and ganglion cells in the INL and GCL, and their processes in strata 1/2, 2/3, and 3/4 of the IPL (Fig. 3B) (Haverkamp and Wässle, 2000, Ghosh et al., 2004). RFP fluorescent processes were in strata 1, 2/3, and 3, and in the OPL. RFP fluorescent processes in strata 2/3 and 3 were fainter in comparison to calretinin fluorescent processes. The small diameter RFP fluorescent cells and their processes in stratum 2/3 were calretinin immunoreactive (Fig. 3B).

Next, we tested for GABA and glycine expression in the RFP fluorescent cells. All RFP fluorescent cells contained GABA immunoreactivity (Fig. 3C, arrowhead), but they did not contain glycine immunoreactivity (Fig. 3D, arrow). These findings are consistent with previous reports on type 1 and 2 DA amacrine cells (Wulle and Wagner, 1990, Nguyen-Legros et al., 1997, Völgyi et al., 1997).

TH-BAC-tdTomato retina—In the TH-BAC-tdTomato retinas there were very few medium to large diameter fluorescent cells with TH immunoreactivity (Fig. 4A, inset). In retinal whole-mount preparations, 0.32% (n=50/15415 cells; 4 retinas; Table 3) of the fluorescent cells contained TH immunoreactivity. Conversely, about 11% (n=50/449 cells; 4 retinas) of the TH-immunoreactive cells expressed tdTomato fluorescence.

Varicose tdTomato fluorescent processes ramified extensively in strata 1, 2/3, 4, and 5 of the IPL, and there were also thin, smooth fluorescent processes in the NFL (Fig. 1B and 4A, bottom). There were fewer fluorescent processes in strata 1 and 2/3 compared to strata 4 and 5 of the IPL (Fig. 1B and 4). tdTomato fluorescent cells with calretinin immunoreactivity were in the INL (not shown) and in the GCL (Fig. 4B) and their co-localized processes were in the OFF sublamina of the IPL.

Overall, calretinin and GABA immunoreactivity was co-localized to about 9% and 8% (n=1587/17303 and 930/12576 cells; 3 retinas) of the total number of tdTomato fluorescent cells, respectively (Fig. 4B and C; Table 3). The majority of the GABA immunoreactive cells were in the GCL (74%) and fewer (9%) were in the INL (Table 3). The small diameter cells in the GCL (6.86 ± 1.06 μm; n=139 cells; 2 retinas; Table 2) were identified as displaced amacrine cells based on their expression of GABA immunoreactivity (Fig. 4C). The medium diameter (9.10 ± 0.57 μm; n=20 cells; 2 retinas; Table 2) cells in the INL (Fig. 5A, *left panel*, arrows) were GABA immunoreactive, and had processes that ramified extensively in the OFF sublamina of the IPL. These wide-field amacrine cells had field sizes that were greater than 300 μm (n=10 cells; 2 retinas) in diameter and were found throughout the retina, but were infrequent overall (Fig. 5A, *left panel*, arrows).

About 85% (n=40/47 cells; 2 retinas; Table 3) of the tdTomato-expressing cells in the INL contained glycine immunoreactivity (Fig. 4D, arrowhead), and displayed a stratification pattern in the IPL similar to AII amacrine cells (Fig. 1B and 4D) (Wässle et al., 1995, Menger et al., 1998, Massey and Mills, 1999). In the proximal INL, small diameter (6.48 ± 1.04 μm; n=300 cells; 2 retinas; Table 2) cells were characterized by lobular appendages in the OFF sublamina, and varicose arborizations in the ON sublamina of the IPL (Fig. 4 and 5A, *right panel*). These findings support the suggestion that AII amacrine cells are labeled in

this line. AII amacrine cells in whole mounted retinas were in clusters in all retinal regions (Fig. 5A, *right panel*). Medium somal diameter cells in the GCL measured 10.98 ± 2.24 μm (n=719 cells; 3 retinas; Table 2). About 25% of the fluorescent cells were not immunoreactive for GABA or glycine, and had smooth axon-like processes that extended along the NFL, suggesting they are ganglion cells (Fig. 5B, *left*). To test this possibility, whole-mounted retinas were immunostained with an antibody to RBPMS, a specific marker for retinal ganglion cells (Rodriguez et al., 2014). About 24% of the total tdTomato cells (n=947/3911 cells; 3 retinas) in the GCL contained RBPMS (Table 3; Fig. 5B, *right panel*, arrowheads). Less than 0.5% (n=50/10802 cells; 3 retinas) of the fluorescent cells in the INL contained RBPMS immunoreactivity (Table 3). The tdTomato cells that did not co-localize with GABA, glycine, or RBPMS are less than 5% and 1% of the tdTomato cells in the INL and GCL, respectively. The tdTomato cells that were co-localized with RBPMS immunoreactivity were few overall, and sparsely distributed, with some cell bodies that were in close proximity and others that were further apart (Fig. 5B, *right panel*, arrowheads). The somal size of the tdTomato cells that co-localized with RBPMS immunoreactivity in the INL ranged from 7.92 to 15.29 μm, and averaged 10.02 ± 2.25 μm (n=50 cells; 3 retinas; Figure 6A). Those in the GCL ranged from 7.44 to 19.27 μm, and averaged 10.98 ± 2.24 μm (n=719 cells; 3 retinas; Figure 6B). Collectively these findings indicate that multiple ganglion cell subtypes are likely to be labeled in this line (Sun et al., 2002, Völgyi et al., 2009).

TH-tdTomato retina—In vertical sections of TH-tdTomato retinas there were few medium to large diameter fluorescent cells with TH immunoreactivity (Fig. 7A inset). Numerous fluorescent cells also contained calretinin in both the INL and GCL, and their processes ramified in a distinct band in stratum 2/3 of the IPL, and weaker bands in strata 1 and 4 of the IPL (Fig. 7B, D). tdTomato cells were positive for GABA immunoreactivity (Fig. 7C) in the INL and GCL, but lacked glycine immunoreactivity (Fig. 7D).

The small diameter cells (6.76 ± 0.99 μm; n=236 cells; 2 retinas; Table 2) in the INL were monostratified cells with processes in stratum 1 or 2/3 (Fig. 7B). The small diameter cells in the GCL (7.25 ± 1.02 μm; n=36; 2 retinas; Table 2) had processes that primarily ramified in stratum 2/3 (not shown), similar to type 2 DA amacrine cells. The medium diameter somata (10.11 ± 1.49 μm; n=84 cells; 2 retinas; Table 2) in the proximal INL had multiple primary processes that formed a thick band in the ON-OFF sublamina and other processes that were distributed throughout the IPL (Fig. 1C and 7). The medium diameter somata (10.34 ± 1.40 μm; n=44 cells; 2 retinas; Table 2) in the GCL primarily ramified in stratum 4 of the IPL (Fig 1C and 7).

In retinal whole mounts, about 81% (n=1483/1829 cells; 3 retinas; Table 3) of the fluorescent somata contained calretinin immunoreactivity. The majority (89%) of the tdTomato fluorescent somata in the INL (Fig. 8B) and GCL (Fig. 8C) contained GABA immunoreactivity (n=221/248 cells; 2 retinas; Table 3). In whole-mounted retinas very few cells in the INL (1.5%; n=16/1062 cells; 2 retinas; Table 3) contained glycine immunoreactivity (Fig. 8A, arrows).

There were several types of tdTomato cells that contain GABA immunoreactivity, and a few that contained ChAT (Fig. 9A and B) or TH immunoreactivity (Fig. 9C). ChAT immunoreactivity was in about 6% (n=63/1038 cells; 2 retinas; Table 3) of the tdTomato fluorescent cells. About 6% (n=141/2238 cells; 4 retinas; Table 3) of the fluorescent cells contained TH immunoreactivity (Fig. 98C arrow vs. arrowheads). Conversely, about ~28% (n=141/507 cells; 4 retinas, Table 3) of the TH-immunoreactive cells expressed tdTomato fluorescence. In addition, another group of GABA immunoreactive cells in the TH-tdTomato retinas was the wide-field amacrine cells. In order to illustrate the individual morphological attributes of the wide-field amacrine cell types labeled in this mouse line, we performed intracellular injections of Neurobiotin into tdTomato-expressing cells in whole mount preparations. At least four types of polyaxonal amacrine cells contained tdTomato fluorescence. Classification of the polyaxonal amacrine cells was determined based on their cellular localization, dendritic branching, and axon-like processes (Famiglietti, 1992a, b, Völgyi et al., 2001, Wright and Vaney, 2004, Völgyi et al., 2009, Greschner et al., 2014). In the INL, there were two types of polyaxonal amacrine cells: one that had radially oriented processes with prominent varicosities, which arborized in stratum 2 of the IPL (Fig. 10A), and the second type corresponded to type 1 DA amacrine cells, which arborized in stratum 1 of the IPL (Fig. 10A′). Cellular reconstructions of the Neurobiotin injected cells highlighted the morphological differences between the two cell types; the radially oriented polyaxonal amacrine cells had prominent thin and smooth, axon-like processes that extended 1–2 mm from the cell body (Fig. 10A″) and the type 1 DA amacrine cells had wide-field processes that extended about 1 mm in diameter from the cell body (Fig. 10A‴). The GCL also had two types of polyaxonal amacrine cells, which are differentiated by asymmetrical (Fig. 10B) and radially oriented (Fig. 10B′) processes. The processes of the asymmetrical polyaxonal amacrine cells had numerous spines (Fig. 10B) and tended to have long axon-like processes that spanned the retina, and often they were over 1 mm in length (Fig. 10B″). In contrast, the processes of the radial polyaxonal amacrine cells had numerous varicosities (Fig. 10B′) and they extended about 1 mm in diameter from the cell body (Fig. 10B‴). The processes of both types of displaced polyaxonal amacrine cells arborized in stratum 5 of the IPL (Fig. 10B, B′).

Finally, TH-tdTomato fluorescent somata in the GCL did not contain RBPMS immunoreactivity (not shown), indicating that retinal ganglion cells in the TH-tdTomato retina do not express Cre activity.

DAT-tdTomato retina—Retinas of the DAT-tdTomato line had fluorescent cells primarily in the INL (Fig. 1D, 2D, and 11) and processes in strata 1, 3, 4, and 5 (Fig. 11B). The tdTomato cells were GABA immunoreactive (Fig. 11C), but they were not TH, calretinin, or glycine immunoreactive (Fig. 11A, B, D).

To test whether there are multiple types of labeled amacrine cells, we made intracellular injections of Neurobiotin into tdTomato-expressing cells in retinal whole mount preparations. In the INL, the tdTomato fluorescent cells are predominantly composed of two types of bistratified amacrine cells (Fig. 12A, B) and one type of monostratified amacrine cell (Fig. 12C). The large field bistratified amacrine cells had an average somal diameter of 9.55 ± 0.21 μm (n=3 cells; 2 retinas), and an average dendritic field of 670.00 ± 26.94 μm in

the OFF sublamina and 665.00 ± 33.80 μm in the ON sublamina of the IPL (Fig. 12A, A′). On this basis we classified these bistratified amacrine cells as wide-field amacrine cells. On the other hand, the more frequently occurring medium-field bistratified amacrine cells had an average somal diameter of 11.00 ± 1.55 μm (n=4 cells; 2 retinas), and an average dendritic field size of 388.00 ± 84.24 μm in the OFF sublamina and 297.00 ± 62.65 μm in the ON sublamina of the IPL (Fig. 12B, B′). In addition, the INL had wide-field amacrine cells that arborized in stratum 1 of the IPL (Fig. 12C, C′). This cell had a soma size of 10.6 μm and a dendritic field size of 885.2 μm (n=1 cell; 2 retinas). Finally, in the GCL we found displaced amacrine cells with an average soma size of 10.0 ± 0.28 μm (n=3 cells; 2 retinas) and a smaller dendritic field size (229.00 ± 48.41 μm) compared to the monostratified cells in the INL (Fig. 12D, D′). Together, the analysis of Neurobiotin injected tdTomato fluorescent cells in whole mount retinas and GABA immunoreactivity in the transverse sections suggests that there are multiple amacrine cell types.

Discussion

This study has evaluated Cre-mediated fluorescence in the retinas of three Cre transgenic mouse lines crossed with a tdTomato reporter line (Ai14) (Savitt et al., 2005, Bäckman et al., 2006, Gong et al., 2007, Madisen et al., 2010). These Cre-expressing retinas either lacked or had a low percentage of type 1 DA amacrine cells. In comparison, the previously characterized TH-RFP, TH-PLAP and TH-GFP mouse lines, only have labeled type 1 and 2 DA amacrine cells (Gustincich et al., 1997, Matsushita et al., 2002, Zhang et al., 2004, Knop et al., 2011).

The cellular expression patterns in retinas of many transgenic lines, including both Cre and BAC-Cre lines (Rowan and Cepko, 2004, Haverkamp et al., 2009, Lu et al., 2009, Siegert et al., 2009, Ivanova et al., 2010) includes: 1) the ectopic expression of the transgene in cell types that do not endogenously express the gene, 2) the incomplete expression of the transgene in its endogenous cell types, or 3) a combination of both (Gong et al., 2007, Haverkamp et al., 2009, Ivanova et al., 2010). These patterns of Cre-induced tdTomato fluorescence are also seen in our screen of the dopamine transmitter-related Cre lines: the TH-BAC- and TH-tdTomato retinas had incomplete labeling of type 1 DA amacrine cells as well as numerous other ectopically labeled amacrine cells, and the DAT-tdTomato retina had bistratified and monostratified amacrine cell types, but no labeling of the type 1 DA amacrine cells.

Transgenic expression of fluorescent reporters

TH-RFP—The fluorescent labeling pattern in the TH-RFP transgenic mouse line is similar to previous findings by Zhang et al. (2004). The TH-RFP line contains type 1 DA amacrine cells, which were defined by their characteristic morphology, including a medium to large soma, extensive wide-ranging arborizations in stratum 1 of the IPL, and TH (Fig. 3A) and GABA (Fig. 3C) immunoreactivity. In addition, TH-RFP retinas contain type 2 DA amacrine cells. However, type 2 DA amacrine cells in mouse retina, have not been reported to contain TH immunoreactivity (Zhang et al., 2004) suggesting an absence or a very low level of TH protein (Stuber et al., 2015).

TH-BAC-, TH-, and DAT-Cre lines

TH-BAC-tdTomato—The TH-BAC-Cre line was generated by inserting a Cre gene into the intron at the start of a *Th* gene coding region (ATG) (<150kb) into a BAC vector (Gong et al., 2007). Cre expression was in TH-immunoreactive neurons in all of the catecholamine cell groups (Gong et al., 2007). In addition, Cre-induced EGFP fluorescence was in some striatal and hypothalamic neurons that were not TH-immunoreactive (Komori et al., 1991, Marin et al., 2005, Gong et al., 2007). Interestingly, other lines in this series, including the ChAT, Slc6a4, Drd1a and Drd2, which were produced by the same BAC-Cre strategy, also showed ectopic cell expression in the central nervous system (Gong et al., 2007). Ectopic Cre activity was also common in our study of the TH-BAC-tdTomato retinas. In contrast to the rest of the central nervous system, TH-BAC-tdTomato retinas had a very low percentage of Cre-expressing TH-immunoreactive cells. However, there were numerous other amacrine cells, and a small number of ganglion cells with Cre activity.

Fluorescent cells in the TH-BAC-tdTomato retinas were immunoreactive for the amacrine cell transmitters, GABA and glycine, and the ganglion cell marker, RBPMS (Rodriguez et al., 2014). The majority (85%) of the fluorescent amacrine cells in the INL were the glycine-immunoreactive AII amacrine cells (Table 3) based on their morphology (Wässle et al., 1995, MacNeil and Masland, 1998, Menger et al., 1998, Massey and Mills, 1999). In addition, the co-expression of tdTomato fluorescence and RBPMS-immunoreactivity indicates the presence of labeled retinal ganglion cells in the TH-BAC-tdTomato line. These cells comprise a low percentage (less than 0.5% in the INL and ~24% in the GCL, Table 3) of the total number of Cre-expressing retinal cells. The range of the soma diameters (7.44 to 19.27 μm; n=719 cells; 3 retinas) of the labeled cells in the GCL and the distribution of labeled dendrites to all IPL laminae suggests multiple fluorescent ganglion cell types (Sun et al., 2002, Völgyi et al., 2009). These findings suggest that there are multiple labeled ganglion cell types in this line, and reliable identification of specific ganglion cell types would be difficult in this line. However, this line would useful for studying AII amacrine cells, due to their robust labeling.

The remaining cells that do not co-localize with GABA, glycine or RBPMS, which make up less than 6% of the total tdTomato cells, possibly have a low level of GABA, glycine or RBPMS, and the strong tdTomato signal possibly masked the antibody fluorescence in the cells. Another possibility is that these cells may be non-GABA or –glycine amacrine cells (Kay et al., 2011b).

TH-tdTomato—The TH-Cre line transgene used in this study consists of a Cre gene driven by a 9 kb genomic fragment of the rat TH promoter. This line was obtained from the Jackson Laboratory (Savitt et al., 2005). The initial characterization of this line showed Cre-induced hPLAP activity and GFP expression in TH-immunoreactive neurons in all of the catecholaminergic cell groups examined (Savitt et al., 2005). In the retina, Cre activity was also reported in amacrine cells with processes that ramify extensively and broadly in the middle of the IPL. The authors noted that the pattern of cellular expression of Cre activity in the retina varied in the five TH-Cre lines they generated for their studies. In another TH-Cre line, also generated using the same 9 kb TH rat genomic fragment, type 1 DA amacrine cells

were shown to express Cre and TH immunoreactivity, and hPLAP activity (Gelman et al., 2003). In a TH-Cre line generated with an IRES-Cre sequence inserted into the 3′ untranslated region of the *TH* gene, Cre activity was expressed by some cells in the GCL (Lindeberg et al., 2004). In contrast to these earlier findings, we observed a more complex cellular labeling pattern than the initial descriptions of the TH-Cre line (see Fig. 4 (Gelman et al., 2003)).

In these TH-Cre lines, Cre activity was in many but not all TH immunoreactive neurons in the dopamine-containing cell groups, and in addition, Cre activity was in many neurons in regions that do not contain TH immunoreactive neurons in the adult central nervous system (Min et al., 1994, Gelman et al., 2003, Lindeberg et al., 2004, Savitt et al., 2005, Lammel et al., 2015, Stuber et al., 2015). Regions with ectopic expression of Cre activity include the interpeduncular nucleus, supramammillary nucleus, and midline ventral tegmental area (VTA) regions of the posterior and anterior ventral midbrain (Lindeberg et al., 2004, Savitt et al., 2005, Lammel et al., 2015). In the retina of the TH-Cre line evaluated in this study, Cre activity was in a small percentage of the TH-immunoreactive amacrine cells and most of the Cre activity was in in non-TH immunoreactive amacrine cells.

In the TH-tdTomato retina, Cre-dependent fluorescent cell bodies are in the INL and GCL, and their processes ramify in strata 1, 2/3, and 4 of the IPL. TH-tdTomato fluorescent cells contained GABA, TH, ChAT and calretinin immunoreactivity. These results indicate multiple cell types, with ~89% of the total number of tdTomato fluorescent cells containing GABA immunoreactivity. Possible explanations for the lack of GABA or glycine immunoreactivity in a small percentage of tdTomato fluorescent amacrine cells could be that they have low levels of the neurotransmitters, which cannot be detected by antibodies, or these amacrine cells are members of the recently described non-GABA or -glycine immunoreactive amacrine cell group (Kay et al., 2011b). The most prominently labeled GABA-immunoreactive cell types were the polyaxonal amacrine cells (Fig. 12), which could be readily identified in retinal whole-mounts based on their somal size and the extensive arborization of their processes (Lin and Masland, 2006). The polyaxonal amacrine cell type that is localized to the INL and stratifies in stratum 2 of the IPL is most similar to the WA2 amacrine cell type (Lin and Masland, 2006). Both of these cells share multiple features including the same somata localization in the INL, level of IPL stratification (stratum 2), and axonal field size (~2–3 mm) (Lin and Masland, 2006). The other two types of displaced polyaxonal amacrine cells that stratify in stratum 5 of the IPL have not been reported in previous studies. This TH-Cre line will be highly useful for future studies of polyaxonal amacrine cells with the aim to better define their biophysical properties, connectivity and functional relationships.

DAT-tdTomato—The DAT-Cre line used in this study was generated by inserting an IRES sequence followed by the *Cre* gene into the 3′ untranslated region of the *Dat* gene (Bäckman et al., 2006). Cre-mediated fluorescence, and Cre and DAT immunoreactivity were restricted to dopaminergic neurons in the VTA, substantia nigra pars compacta (SNpc) and retrorubral field, and weak Cre activity was also in neurons in the periglomerular layer of the olfactory bulb, and in some weakly expressing neurons in the hypothalamus (Bäckman et al., 2006, Lammel et al., 2015). In a DAT-BAC-iCre line, Cre activity was also confined to TH

immunoreactive neurons in all of the dopaminergic groups in the central nervous system (Turiault et al., 2007). In addition, in a third DAT-Cre line with the Cre gene inserted downstream of the DAT promoter region, Cre immunoreactivity and activity was mainly in TH immunoreactive neurons in the VTA and SNpc, and in a few neurons in the cortex, septum and hippocampus (Zhuang et al., 2005). TH immunoreactive cells are not reported in cortex, septum and hippocampus of the adult central nervous system (Chinta and Andersen, 2005, Prakash and Wurst, 2006) indicating sparse ectopic Cre activity in this particular line.

Unlike the findings in the central nervous system of the DAT-Cre lines, where Cre activity is reported to be predominantly or exclusively located to neurons in the dopamine-containing cell groups (Zhuang et al., 2005, Bäckman et al., 2006, Turiault et al., 2007, Lammel et al., 2015), in the retina, the predominant type 1 DA amacrine cell does not express detectable levels of the tdTomato reporter, suggesting Cre activity is absent in these cells. The lack of Cre expression in type 1 DA amacrine cells is surprising, since DAT immunoreactivity is in type 1 DA amacrine cells in the rat and bullfrog retina (Cheng et al., 2006), and there is high affinity uptake of dopamine by type 1 DA amacrine cells in the cat and rabbit retina (Ehinger and Floren, 1978, Pourcho, 1982, Tauchi et al., 1990).

In contrast, the present study shows that the DAT-tdTomato retinas robustly express Cre-mediated fluorescence predominantly in two bistratified amacrine cell types and two monostratified amacrine cell types. The tdTomato fluorescent cell bodies contained GABA immunoreactivity, but lacked TH and glycine immunoreactivity (Fig. 11 and 12) (Gustincich et al., 1997, Zhang et al., 2004, Sarthy et al., 2007, Knop et al., 2011, Brüggen et al., 2014, Knop et al., 2014).

Retinal sections from the DAT-tdTomato line revealed two predominant bands of stratification (stratum 1 and strata 3, 4, and 5) in the IPL (Fig. 1D, 11B, and 12), and retinal whole mounts had an average of 646 ± 160 fluorescent cells/mm^2 of retina (Fig. 2D). There were two bistratified amacrine cells and they differed from the previously reported A1 bistratified cells because the A1 somata are in the GCL and their processes primarily stratify near the GCL and few reach out towards the INL (Badea and Nathans, 2004). The small field size bistratified amacrine cells (Fig. 12B) in the DAT-tdTomato retina are similar to medium-field bistratified amacrine cells, which have processes that stratify in two principal laminae and have a field size of 150–200 μm (Badea and Nathans, 2004). Although the presence of a diversity of medium-field bistratified amacrine cells has been observed (MacNeil and Masland, 1998, Badea and Nathans, 2004, Haverkamp and Wässle, 2004), unique to this DAT-tdTomato mouse line is tdTomato expression in wide-field bistratified amacrine cells (Fig. 12A). The wide-field bistratified amacrine cell of the DAT-tdTomato mouse line is most similar in morphology to the asymmetrical bistratified amacrine cell in rabbit retina (MacNeil and Masland, 1998). However, the asymmetrical bistratified amacrine cell arborizes in strata 2 and 4 of the IPL, and has a noticeably smaller field size. This finding indicates the DAT-tdTomato retinas contain a novel wide-field bistratified amacrine cell.

In addition to the observation of bistratified amacrine cells, the DAT-tdTomato line has at least two populations of monostratified amacrine cells. The first monostratified amacrine

cell was in the INL, and its processes ramifed in stratum 1 of the IPL (Fig. 12C). Based on Neurobiotin intracellular injections, these cells have a large dendritic field size and are wide-field amacrine cells. These cells are similar in morphology and stratification pattern to the stratum 1 amacrine cell identified in rabbit retina (Vaney, 1986, Xin and Bloomfield, 1997, Li et al., 2002). In addition, the stratum 1 monostratified amacrine cell is similar to the WA-1 amacrine cells in the mouse retina, although the WA-1 is always displaced to the GCL (Lin and Masland, 2006). The second type of monostratified amacrine cell was displaced to the GCL (Fig. 12D). These cells have a medium-field dendritic field diameter (229 ± 48.41 μm), and a morphology and stratification pattern similar to the previously described for DA1 cells in the guinea pig retina (Kao and Sterling, 2006). However, this particular morphology and stratification pattern has not been described in mouse retinas, thus making it difficult to make an accurate comparison. Therefore, this DAT-tdTomato line showed multiple wide-field bistratified and monostratified amacrine cell types.

Ectopic and incomplete expression of Cre-induced fluorescence in the retina

All three Cre lines were characterized by a low percentage or lack of type 1 DA amacrine cells with Cre-induced fluorescence (Fig. 4A, 7A, and 9A). In these retinas, the majority of Cre-expressing cells were glycine- or GABA-immunoreactive amacrine cells. In addition, in the TH-BAC-tdTomato line, a small number of ganglion cells expressed Cre-dependent fluorescence. The TH-BAC- and TH-Cre retinas also showed partial penetrance of Cre into type 1 DA amacrine cells. The limited Cre-mediated fluorescence in type 1 DA amacrine cells may also be due to a low number of copies of Cre constructs knocked into the genome compared to the labeling of a majority of TH immunoreactive cells in the TH-RFP, TH-PLAP and TH-GFP retinas (Heintz, 2001, Gelman et al., 2003, Lindeberg et al., 2004, Savitt et al., 2005, Zhuang et al., 2005, Bäckman et al., 2006, Gong et al., 2007, Lammel et al., 2015).

Ectopic expression of Cre activity in amacrine cells is a predominant feature of the DAT-, TH-BAC- and TH-Cre lines. One possible reason is that there is a positional influence of the exogenous DAT or TH genomic DNA inserts, in which their integration into the genome changes endogenous expression patterns (Gong et al., 2007). Another factor that may influence ectopic Cre activity is the lack of regulatory regions to switch off the *Th* gene (Min et al., 1994, Gelman et al., 2003). In addition, perhaps there is a retina-specific regulatory element lacking in these constructs or epigenetic factors that are needed to properly direct DA amacrine cell expression (Telese et al., 2013). Ectopic expression can also be a result of the transient expression of the *Dat* or *Th* gene during retinal development. For instance, in the central nervous system, transient, developmental expression of *Th* gene occurs in the same regions showing ectopically Cre-expressing cells in mature tissue (Komori et al., 1991, Gong et al., 2002, Marin et al., 2005, Gong et al., 2007). It is possible the transient expression of the *Th* gene in amacrine cell progenitors accounts for the multiple ectopic labeled amacrine cell types observed in the TH- and TH-BAC-Cre retinas.

Conclusion

Retinas of the three Cre lines characterized in this report can serve as a platform for future investigations of amacrine cells. The TH-BAC-tdTomato retina can be better used to study

AII amacrine cells. Retinas of TH-tdTomato mouse line can be used for studying polyaxonal wide-field amacrine cells, including their synaptic partners, intrinsic properties, and specific functions in visual processing. The DAT-tdTomato retina contains multiple types of labeled wide-field bistratified and monostratified amacrine cells.

Acknowledgments

We thank Dr. Arlene Hirano for her comments and discussion on this project and manuscript.

Support and grant information:

Support for these studies was from NIH EY04067 (NCB), P30DK41301 (NCB), a VA Merit Review (NCB), NIH T32 EY007026 (HEV), Whitcome Summer Undergraduate Research Fellowship (CNH) and NIH EY09256 (DGM). NCB is a VA Career Research Scientist.

References

Aung MH, Park HN, Han MK, Obertone TS, Abey J, Aseem F, Thule PM, Iuvone PM, Pardue MT. Dopamine deficiency contributes to early visual dysfunction in a rodent model of type 1 diabetes. J Neurosci. 2014; 34:726–736. [PubMed: 24431431]

Bäckman CM, Malik N, Zhang Y, Shan L, Grinberg A, Hoffer BJ, Westphal H, Tomac AC. Characterization of a mouse strain expressing Cre recombinase from the 3′ untranslated region of the dopamine transporter locus. Genesis. 2006; 44:383–390. [PubMed: 16865686]

Badea TC, Nathans J. Quantitative analysis of neuronal morphologies in the mouse retina visualized by using a genetically directed reporter. J Comp Neurol. 2004; 480:331–351. [PubMed: 15558785]

Ballesta J, Terenghi G, Thibault J, Polak JM. Putative dopamine-containing cells in the retina of seven species demonstrated by tyrosine hydroxylase immunocytochemistry. Neuroscience. 1984; 12:1147–1156. [PubMed: 6148714]

Boycott BB, Wässle H. The morphological types of ganglion cells of the domestic cat's retina. J Physiol. 1974; 240:397–419. [PubMed: 4422168]

Brecha N, Karten HJ, Laverack C. Enkephalin-containing amacrine cells in the avian retina: immunohistochemical localization. Proc Natl Acad Sci U S A. 1979; 76:3010–3014. [PubMed: 379870]

Brecha NC, Oyster CW, Takahashi ES. Identification and characterization of tyrosine hydroxylase immunoreactive amacrine cells. Invest Ophthalmol Vis Sci. 1984; 25:66–70. [PubMed: 6142028]

Brüggen B, Meyer A, Boven F, Weiler R, Dedek K. Type 2 wide-field amacrine cells in TH::GFP mice show a homogenous synapse distribution and contact small ganglion cells. Eur J Neurosci. 2014

Casini G, Brecha NC. Vasoactive intestinal polypeptide-containing cells in the rabbit retina: immunohistochemical localization and quantitative analysis. J Comp Neurol. 1991; 305:313–327. [PubMed: 2026790]

Casini G, Rickman DW, Brecha NC. AII amacrine cell population in the rabbit retina: identification by parvalbumin immunoreactivity. J Comp Neurol. 1995; 356:132–142. [PubMed: 7629307]

Cheng Z, Zhong YM, Yang XL. Expression of the dopamine transporter in rat and bullfrog retinas. Neuroreport. 2006; 17:773–777. [PubMed: 16708013]

Chinta SJ, Andersen JK. Dopaminergic neurons. Int J Biochem Cell Biol. 2005; 37:942–946. [PubMed: 15743669]

Contini M, Lin B, Kobayashi K, Okano H, Masland RH, Raviola E. Synaptic input of ON-bipolar cells onto the dopaminergic neurons of the mouse retina. J Comp Neurol. 2010; 518:2035–2050. [PubMed: 20394057]

Dacey DM. The dopaminergic amacrine cell. J Comp Neurol. 1990; 301:461–489. [PubMed: 1979792]

Dhande OS, Estevez ME, Quattrochi LE, El-Danaf RN, Nguyen PL, Berson DM, Huberman AD. Genetic dissection of retinal inputs to brainstem nuclei controlling image stabilization. J Neurosci. 2013; 33:17797–17813. [PubMed: 24198370]

Ehinger B, Floren I. Quantitation of the uptake of indoleamines and dopamine in the rabbit retina. Exp Eye Res. 1978; 26:1–11. [PubMed: 624320]

Famiglietti EV. Polyaxonal amacrine cells of rabbit retina: PA2, PA3, and PA4 cells. Light and electron microscopic studies with a functional interpretation. J Comp Neurol. 1992a; 316:422–446. [PubMed: 1374438]

Famiglietti EV. Polyaxonal amacrine cells of rabbit retina: size and distribution of PA1 cells. J Comp Neurol. 1992b; 316:406–421. [PubMed: 1374437]

Farrow K, Teixeira M, Szikra T, Viney TJ, Balint K, Yonehara K, Roska B. Ambient illumination toggles a neuronal circuit switch in the retina and visual perception at cone threshold. Neuron. 2013; 78:325–338. [PubMed: 23541902]

Feigenspan A, Gustincich S, Bean BP, Raviola E. Spontaneous activity of solitary dopaminergic cells of the retina. J Neurosci. 1998; 18:6776–6789. [PubMed: 9712649]

Feigenspan A, Gustincich S, Raviola E. Pharmacology of GABA(A) receptors of retinal dopaminergic neurons. J Neurophysiol. 2000; 84:1697–1707. [PubMed: 11024062]

Gelman DM, Noain D, Avale ME, Otero V, Low MJ, Rubinstein M. Transgenic mice engineered to target Cre/loxP-mediated DNA recombination into catecholaminergic neurons. Genesis. 2003; 36:196–202. [PubMed: 12929090]

Ghosh KK, Bujan S, Haverkamp S, Feigenspan A, Wässle H. Types of bipolar cells in the mouse retina. J Comp Neurol. 2004; 469:70–82. [PubMed: 14689473]

Gong S, Doughty M, Harbaugh CR, Cummins A, Hatten ME, Heintz N, Gerfen CR. Targeting Cre recombinase to specific neuron populations with bacterial artificial chromosome constructs. J Neurosci. 2007; 27:9817–9823. [PubMed: 17855595]

Gong S, Yang XW, Li C, Heintz N. Highly efficient modification of bacterial artificial chromosomes (BACs) using novel shuttle vectors containing the R6Kgamma origin of replication. Genome Res. 2002; 12:1992–1998. [PubMed: 12466304]

Greschner M, Field GD, Li PH, Schiff ML, Gauthier JL, Ahn D, Sher A, Litke AM, Chichilnisky EJ. A polyaxonal amacrine cell population in the primate retina. J Neurosci. 2014; 34:3597–3606. [PubMed: 24599459]

Gustincich S, Feigenspan A, Wu DK, Koopman LJ, Raviola E. Control of dopamine release in the retina: a transgenic approach to neural networks. Neuron. 1997; 18:723–736. [PubMed: 9182798]

Hammen GF, Turaga D, Holy TE, Meeks JP. Functional organization of glomerular maps in the mouse accessory olfactory bulb. Nat Neurosci. 2014; 17:953–961. [PubMed: 24880215]

Haverkamp S, Inta D, Monyer H, Wässle H. Expression analysis of green fluorescent protein in retinal neurons of four transgenic mouse lines. Neuroscience. 2009; 160:126–139. [PubMed: 19232378]

Haverkamp S, Wässle H. Immunocytochemical analysis of the mouse retina. J Comp Neurol. 2000; 424:1–23. [PubMed: 10888735]

Haverkamp S, Wässle H. Characterization of an amacrine cell type of the mammalian retina immunoreactive for vesicular glutamate transporter 3. J Comp Neurol. 2004; 468:251–263. [PubMed: 14648683]

Heintz N. BAC to the future: the use of bac transgenic mice for neuroscience research. Nat Rev Neurosci. 2001; 2:861–870. [PubMed: 11733793]

Hirano AA, Brandstätter JH, Brecha NC. Cellular distribution and subcellular localization of molecular components of vesicular transmitter release in horizontal cells of rabbit retina. J Comp Neurol. 2005; 488:70–81. [PubMed: 15912504]

Hirasawa H, Betensky RA, Raviola E. Corelease of dopamine and GABA by a retinal dopaminergic neuron. J Neurosci. 2012; 32:13281–13291. [PubMed: 22993444]

Hirasawa H, Puopolo M, Raviola E. Extrasynaptic release of GABA by retinal dopaminergic neurons. J Neurophysiol. 2009; 102:146–158. [PubMed: 19403749]

Ivanova E, Hwang GS, Pan ZH. Characterization of transgenic mouse lines expressing Cre recombinase in the retina. Neuroscience. 2010; 165:233–243. [PubMed: 19837136]

Kao YH, Sterling P. Displaced GAD65 amacrine cells of the guinea pig retina are morphologically diverse. Vis Neurosci. 2006; 23:931–939. [PubMed: 17266785]

Karten HJ, Brecha N. Localisation of substance P immunoreactivity in amacrine cells of the retina. Nature. 1980; 283:87–88. [PubMed: 6985713]

Kay JN, De la Huerta I, Kim IJ, Zhang Y, Yamagata M, Chu MW, Meister M, Sanes JR. Retinal ganglion cells with distinct directional preferences differ in molecular identity, structure, and central projections. J Neurosci. 2011a; 31:7753–7762. [PubMed: 21613488]

Kay JN, Voinescu PE, Chu MW, Sanes JR. Neurod6 expression defines new retinal amacrine cell subtypes and regulates their fate. Nat Neurosci. 2011b; 14:965–972. [PubMed: 21743471]

Kim IJ, Zhang Y, Meister M, Sanes JR. Laminar restriction of retinal ganglion cell dendrites and axons: subtype-specific developmental patterns revealed with transgenic markers. J Neurosci. 2010; 30:1452–1462. [PubMed: 20107072]

Knop GC, Feigenspan A, Weiler R, Dedek K. Inputs underlying the ON-OFF light responses of type 2 wide-field amacrine cells in TH::GFP mice. J Neurosci. 2011; 31:4780–4791. [PubMed: 21451016]

Knop GC, Pottek M, Monyer H, Weiler R, Dedek K. Morphological and physiological properties of enhanced green fluorescent protein (EGFP)-expressing wide-field amacrine cells in the ChAT-EGFP mouse line. Eur J Neurosci. 2014; 39:800–810. [PubMed: 24299612]

Kolb H, Nelson R. Amacrine cells of the cat retina. Vision Res. 1981; 21:1625–1633. [PubMed: 7336596]

Kolb H, Nelson R, Mariani A. Amacrine cells, bipolar cells and ganglion cells of the cat retina: a Golgi study. Vision Res. 1981; 21:1081–1114. [PubMed: 7314489]

Komori K, Fujii T, Nagatsu I. Do some tyrosine hydroxylase-immunoreactive neurons in the human ventrolateral arcuate nucleus and globus pallidus produce only L-dopa? Neurosci Lett. 1991; 133:203–206. [PubMed: 1687756]

Lammel S, Steinberg EE, Foldy C, Wall NR, Beier K, Luo L, Malenka RC. Diversity of Transgenic Mouse Models for Selective Targeting of Midbrain Dopamine Neurons. Neuron. 2015; 85:429–438. [PubMed: 25611513]

Li W, Zhang J, Massey SC. Coupling pattern of S1 and S2 amacrine cells in the rabbit retina. Vis Neurosci. 2002; 19:119–131. [PubMed: 12385625]

Lin B, Masland RH. Populations of wide-field amacrine cells in the mouse retina. J Comp Neurol. 2006; 499:797–809. [PubMed: 17048228]

Lindeberg J, Usoskin D, Bengtsson H, Gustafsson A, Kylberg A, Soderstrom S, Ebendal T. Transgenic expression of Cre recombinase from the tyrosine hydroxylase locus. Genesis. 2004; 40:67–73. [PubMed: 15452869]

Lu Q, Ivanova E, Pan ZH. Characterization of green fluorescent protein-expressing retinal cone bipolar cells in a 5-hydroxytryptamine receptor 2a transgenic mouse line. Neuroscience. 2009; 163:662–668. [PubMed: 19589372]

MacNeil MA, Heussy JK, Dacheux RF, Raviola E, Masland RH. The shapes and numbers of amacrine cells: matching of photofilled with Golgi-stained cells in the rabbit retina and comparison with other mammalian species. J Comp Neurol. 1999; 413:305–326. [PubMed: 10524341]

MacNeil MA, Masland RH. Extreme diversity among amacrine cells: implications for function. Neuron. 1998; 20:971–982. [PubMed: 9620701]

Madisen L, Zwingman TA, Sunkin SM, Oh SW, Zariwala HA, Gu H, Ng LL, Palmiter RD, Hawrylycz MJ, Jones AR, Lein ES, Zeng H. A robust and high-throughput Cre reporting and characterization system for the whole mouse brain. Nat Neurosci. 2010; 13:133–140. [PubMed: 20023653]

Mariani AP, Hokoç JN. Two types of tyrosine hydroxylase-immunoreactive amacrine cell in the rhesus monkey retina. J Comp Neurol. 1988; 276:81–91. [PubMed: 2903868]

Marin C, Bove J, Serrats J, Cortes R, Mengod G, Tolosa E. The kappa opioid agonist U50,488 potentiates 6-hydroxydopamine-induced neurotoxicity on dopaminergic neurons. Exp Neurol. 2005; 191:41–52. [PubMed: 15589511]

Masland RH. Amacrine cells. Trends Neurosci. 1988; 11:405–410. [PubMed: 2469207]

Masland RH. The fundamental plan of the retina. Nat Neurosci. 2001; 4:877–886. [PubMed: 11528418]

Massey SC, Mills SL. Antibody to calretinin stains AII amacrine cells in the rabbit retina: double-label and confocal analyses. J Comp Neurol. 1999; 411:3–18. [PubMed: 10404104]

Matsushita N, Okada H, Yasoshima Y, Takahashi K, Kiuchi K, Kobayashi K. Dynamics of tyrosine hydroxylase promoter activity during midbrain dopaminergic neuron development. J Neurochem. 2002; 82:295–304. [PubMed: 12124430]

Menger N, Pow DV, Wässle H. Glycinergic amacrine cells of the rat retina. J Comp Neurol. 1998; 401:34–46. [PubMed: 9802699]

Min N, Joh TH, Kim KS, Peng C, Son JH. 5′ upstream DNA sequence of the rat tyrosine hydroxylase gene directs high-level and tissue-specific expression to catecholaminergic neurons in the central nervous system of transgenic mice. Brain Res Mol Brain Res. 1994; 27:281–289. [PubMed: 7898312]

Müller LP, Dedek K, Janssen-Bienhold U, Meyer A, Kreuzberg MM, Lorenz S, Willecke K, Weiler R. Expression and modulation of connexin 30.2, a novel gap junction protein in the mouse retina. Vis Neurosci. 2010a; 27:91–101. [PubMed: 20537217]

Müller LP, Do MT, Yau KW, He S, Baldridge WH. Tracer coupling of intrinsically photosensitive retinal ganglion cells to amacrine cells in the mouse retina. J Comp Neurol. 2010b; 518:4813–4824. [PubMed: 20963830]

Newkirk GS, Hoon M, Wong RO, Detwiler PB. Inhibitory inputs tune the light response properties of dopaminergic amacrine cells in mouse retina. J Neurophysiol. 2013; 110:536–552. [PubMed: 23636722]

Nguyen-Legros J. Functional neuroarchitecture of the retina: hypothesis on the dysfunction of retinal dopaminergic circuitry in Parkinson's disease. Surg Radiol Anat. 1988; 10:137–144. [PubMed: 3135618]

Nguyen-Legros J, Versaux-Botteri C, Savy C. Dopaminergic and GABAergic retinal cell populations in mammals. Microsc Res Tech. 1997; 36:26–42. [PubMed: 9031259]

Oyster CW, Takahashi ES, Cilluffo M, Brecha NC. Morphology and distribution of tyrosine hydroxylase-like immunoreactive neurons in the cat retina. Proc Natl Acad Sci U S A. 1985; 82:6335–6339. [PubMed: 2863820]

Pang JJ, Gao F, Wu SM. Physiological characterization and functional heterogeneity of narrow-field mammalian amacrine cells. J Physiol. 2012; 590:223–234. [PubMed: 22083601]

Pérez de Sevilla Müller L, Shelley J, Weiler R. Displaced amacrine cells of the mouse retina. J Comp Neurol. 2007; 505:177–189. [PubMed: 17853452]

Pohlkamp T, Steller L, May P, Gunther T, Schule R, Frotscher M, Herz J, Bock HH. Generation and characterization of an Nse-CreERT2 transgenic line suitable for inducible gene manipulation in cerebellar granule cells. PLoS One. 2014; 9:e100384. [PubMed: 24950299]

Pourcho RG. Dopaminergic amacrine cells in the cat retina. Brain Res. 1982; 252:101–109. [PubMed: 7172014]

Prakash N, Wurst W. Development of dopaminergic neurons in the mammalian brain. Cell Mol Life Sci. 2006; 63:187–206. [PubMed: 16389456]

Ramirez S, Tonegawa S, Liu X. Identification and optogenetic manipulation of memory engrams in the hippocampus. Front Behav Neurosci. 2013; 7:226. [PubMed: 24478647]

Ramón y Cajal S. La rétine des vertébrés. Cellule Microcircuitry of the cat retina. Annu Rev Neurosci. 1893; 6:149–185.

Rivlin-Etzion M, Zhou K, Wei W, Elstrott J, Nguyen PL, Barres BA, Huberman AD, Feller MB. Transgenic mice reveal unexpected diversity of on-off direction-selective retinal ganglion cell subtypes and brain structures involved in motion processing. J Neurosci. 2011; 31:8760–8769. [PubMed: 21677160]

Robinson S, Todd TP, Pasternak AR, Luikart BW, Skelton PD, Urban DJ, Bucci DJ. Chemogenetic silencing of neurons in retrosplenial cortex disrupts sensory preconditioning. J Neurosci. 2014; 34:10982–10988. [PubMed: 25122898]

Rodriguez AR, de Sevilla Müller LP, Brecha NC. The RNA binding protein RBPMS is a selective marker of ganglion cells in the mammalian retina. J Comp Neurol. 2014; 522:1411–1443. [PubMed: 24318667]

Rowan S, Cepko CL. Genetic analysis of the homeodomain transcription factor Chx10 in the retina using a novel multifunctional BAC transgenic mouse reporter. Dev Biol. 2004; 271:388–402. [PubMed: 15223342]

Sarthy V, Hoshi H, Mills S, Dudley VJ. Characterization of green fluorescent protein-expressing retinal cells in CD 44-transgenic mice. Neuroscience. 2007; 144:1087–1093. [PubMed: 17161542]

Savitt JM, Jang SS, Mu W, Dawson VL, Dawson TM. Bcl-x is required for proper development of the mouse substantia nigra. J Neurosci. 2005; 25:6721–6728. [PubMed: 16033881]

Siegert S, Scherf BG, Del Punta K, Didkovsky N, Heintz N, Roska B. Genetic address book for retinal cell types. Nat Neurosci. 2009; 12:1197–1204. [PubMed: 19648912]

Sternson SM, Roth BL. Chemogenetic tools to interrogate brain functions. Annu Rev Neurosci. 2014; 37:387–407. [PubMed: 25002280]

Stuber GD, Stamatakis AM, Kantak PA. Considerations When Using Cre-Driver Rodent Lines for Studying Ventral Tegmental Area Circuitry. Neuron. 2015; 85:439–445. [PubMed: 25611514]

Sun W, Li N, He S. Large-scale morophological survey of rat retinal ganglion cells. Vis Neurosci. 2002; 19:483–493. [PubMed: 12511081]

Tauchi M, Madigan NK, Masland RH. Shapes and distributions of the catecholamine-accumulating neurons in the rabbit retina. J Comp Neurol. 1990; 293:178–189. [PubMed: 19189710]

Teakle EM, Wildsoet CF, Vaney DI. The spatial organization of tyrosine hydroxylase-immunoreactive amacrine cells in the chicken retina and the consequences of myopia. Vision Res. 1993; 33:2383–2396. [PubMed: 7902629]

Telese F, Gamliel A, Skowronska-Krawczyk D, Garcia-Bassets I, Rosenfeld MG. “Seq-ing” insights into the epigenetics of neuronal gene regulation. Neuron. 2013; 77:606–623. [PubMed: 23439116]

Turiault M, Parnaudeau S, Milet A, Parlato R, Rouzeau JD, Lazar M, Tronche F. Analysis of dopamine transporter gene expression pattern -- generation of DAT-iCre transgenic mice. FEBS J. 2007; 274:3568–3577. [PubMed: 17565601]

Van Hook MJ, Wong KY, Berson DM. Dopaminergic modulation of ganglion-cell photoreceptors in rat. Eur J Neurosci. 2012; 35:507–518. [PubMed: 22304466]

Vaney DI. Morphological identification of serotonin-accumulating neurons in the living retina. Science. 1986; 233:444–446. [PubMed: 3726538]

Vaughn JE, Famiglietti EV Jr, Barber RP, Saito K, Roberts E, Ribak CE. GABAergic amacrine cells in rat retina: immunocytochemical identification and synaptic connectivity. J Comp Neurol. 1981; 197:113–127. [PubMed: 7014659]

Versaux-Botteri C, Nguyen-Legros J, Vigny A, Raoux N. Morphology, density and distribution of tyrosine hydroxylase-like immunoreactive cells in the retina of mice. Brain Res. 1984; 301:192–197. [PubMed: 6145503]

Vlasits AL, Bos R, Morrie RD, Fortuny C, Flannery JG, Feller MB, Rivlin-Etzion M. Visual stimulation switches the polarity of excitatory input to starburst amacrine cells. Neuron. 2014; 83:1172–1184. [PubMed: 25155960]

Voigt T, Wässle H. Dopaminergic innervation of A II amacrine cells in mammalian retina. J Neurosci. 1987; 7:4115–4128. [PubMed: 2891802]

Völgyi B, Chheda S, Bloomfield SA. Tracer coupling patterns of the ganglion cell subtypes in the mouse retina. J Comp Neurol. 2009; 512:664–687. [PubMed: 19051243]

Völgyi B, Pollak E, Buzas P, Gabriel R. Calretinin in neurochemically well-defined cell populations of rabbit retina. Brain Res. 1997; 763:79–86. [PubMed: 9272831]

Völgyi B, Xin D, Amarillo Y, Bloomfield SA. Morphology and physiology of the polyaxonal amacrine cells in the rabbit retina. J Comp Neurol. 2001; 440:109–125. [PubMed: 11745611]

Wässle H. Parallel processing in the mammalian retina. Nat Rev Neurosci. 2004; 5:747–757. [PubMed: 15378035]

Wässle H, Grunert U, Chun MH, Boycott BB. The rod pathway of the macaque monkey retina: identification of AII-amacrine cells with antibodies against calretinin. J Comp Neurol. 1995; 361:537–551. [PubMed: 8550898]

Wässle H, Heinze L, Ivanova E, Majumdar S, Weiss J, Harvey RJ, Haverkamp S. Glycinergic transmission in the Mammalian retina. Front Mol Neurosci. 2009; 2:6. [PubMed: 19924257]

Witkovsky P. Dopamine and retinal function. Doc Ophthalmol. 2004; 108:17–40. [PubMed: 15104164]

Wright LL, Vaney DI. The type 1 polyaxonal amacrine cells of the rabbit retina: a tracer-coupling study. Vis Neurosci. 2004; 21:145–155. [PubMed: 15259566]

Wulle I, Schnitzer J. Distribution and morphology of tyrosine hydroxylase-immunoreactive neurons in the developing mouse retina. Brain Res Dev Brain Res. 1989; 48:59–72. [PubMed: 2568894]

Wulle I, Wagner HJ. GABA and tyrosine hydroxylase immunocytochemistry reveal different patterns of colocalization in retinal neurons of various vertebrates. J Comp Neurol. 1990; 296:173–178. [PubMed: 1972711]

Xiao J, Cai Y, Yen J, Steffen M, Baxter DA, Feigenspan A, Marshak D. Voltage-clamp analysis and computational model of dopaminergic neurons from mouse retina. Vis Neurosci. 2004; 21:835–849. [PubMed: 15733339]

Xin D, Bloomfield SA. Tracer coupling pattern of amacrine and ganglion cells in the rabbit retina. J Comp Neurol. 1997; 383:512–528. [PubMed: 9208996]

Yamagata M, Sanes JR. Expanding the Ig superfamily code for laminar specificity in retina: expression and role of contactins. J Neurosci. 2012; 32:14402–14414. [PubMed: 23055510]

Yonehara K, Farrow K, Ghanem A, Hillier D, Balint K, Teixeira M, Juttner J, Noda M, Neve RL, Conzelmann KK, Roska B. The first stage of cardinal direction selectivity is localized to the dendrites of retinal ganglion cells. Neuron. 2013; 79:1078–1085. [PubMed: 23973208]

Zhang DQ, Belenky MA, Sollars PJ, Pickard GE, McMahon DG. Melanopsin mediates retrograde visual signaling in the retina. PLoS One. 2012; 7:e42647. [PubMed: 22880066]

Zhang DQ, Stone JF, Zhou T, Ohta H, McMahon DG. Characterization of genetically labeled catecholamine neurons in the mouse retina. Neuroreport. 2004; 15:1761–1765. [PubMed: 15257143]

Zhang DQ, Zhou TR, McMahon DG. Functional heterogeneity of retinal dopaminergic neurons underlying their multiple roles in vision. J Neurosci. 2007; 27:692–699. [PubMed: 17234601]

Zhu B, Straznicky C. Dendritic morphology and retinal distribution of tyrosine hydroxylase-like immunoreactive amacrine cells in Bufo marinus. Anat Embryol (Berl). 1990; 181:365–371. [PubMed: 1971740]

Zhu H, Pleil KE, Urban DJ, Moy SS, Kash TL, Roth BL. Chemogenetic inactivation of ventral hippocampal glutamatergic neurons disrupts consolidation of contextual fear memory. Neuropsychopharmacology. 2014a; 39:1880–1892. [PubMed: 24525710]

Zhu H, Roth BL. Silencing synapses with DREADDs. Neuron. 2014; 82:723–725. [PubMed: 24853931]

Zhu Y, Xu J, Hauswirth WW, DeVries SH. Genetically targeted binary labeling of retinal neurons. J Neurosci. 2014b; 34:7845–7861. [PubMed: 24899708]

Zhuang X, Masson J, Gingrich JA, Rayport S, Hen R. Targeted gene expression in dopamine and serotonin neurons of the mouse brain. J Neurosci Methods. 2005; 143:27–32. [PubMed: 15763133]

Highlights

1. TH-RFP retinas only express fluorescently labeled type 1 and 2 dopamine (DA) amacrine cells.
2. TH-BAC-tdTomato retinas mainly express fluorescently labeled AII amacrine cells, and a few type 1 DA amacrine cells.
3. TH-tdTomato retinas express fluorescently labeled GABA-containing amacrine cells, including polyaxonal amacrine cells.
4. DAT-tdTomato retinas express fluorescently labeled two monostratified and two bistratified amacrine cell types.

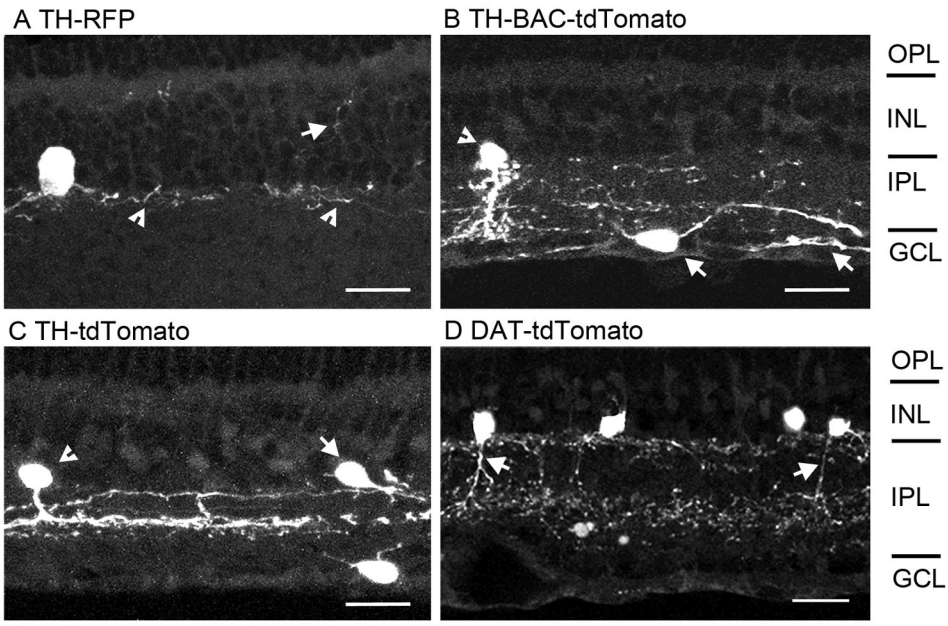

Figure 1. Transgene reporter expression in four transgenic catecholamine-related mouse lines

RFP and tdTomato expression driven by catecholamine specific promoters displayed a heterogeneous labeling of amacrine cells in the retina. **(A)** RFP expression is limited to a subset of amacrine cells in the INL and their processes in stratum 1 of the IPL (arrowheads) and the OPL (arrows). **(B)** TH-BAC-tdTomato line had transgene expression in narrow-field amacrine cells (arrowhead), medium diameter amacrine cells, and putative ganglion cells and their axons in the NFL (arrows). tdTomato expression in the processes was distributed throughout the IPL. **(C)** TH-tdTomato reporter expression was in small- and medium-sized somata in the INL and GCL. There were three primary bands of labeling in the IPL. **(D)** DAT-tdTomato line had tdTomato expression in medium diameter amacrine cells in the INL. tdTomato expression in the processes was distributed in strata 1, 3, 4, and 5 of the IPL. OPL: outer plexiform layer. IPL: inner plexiform layer. INL: inner plexiform layer. GCL: ganglion cell layer RFP: red fluorescent protein. DAT: dopamine transporter. Scale bar: 20 μm.

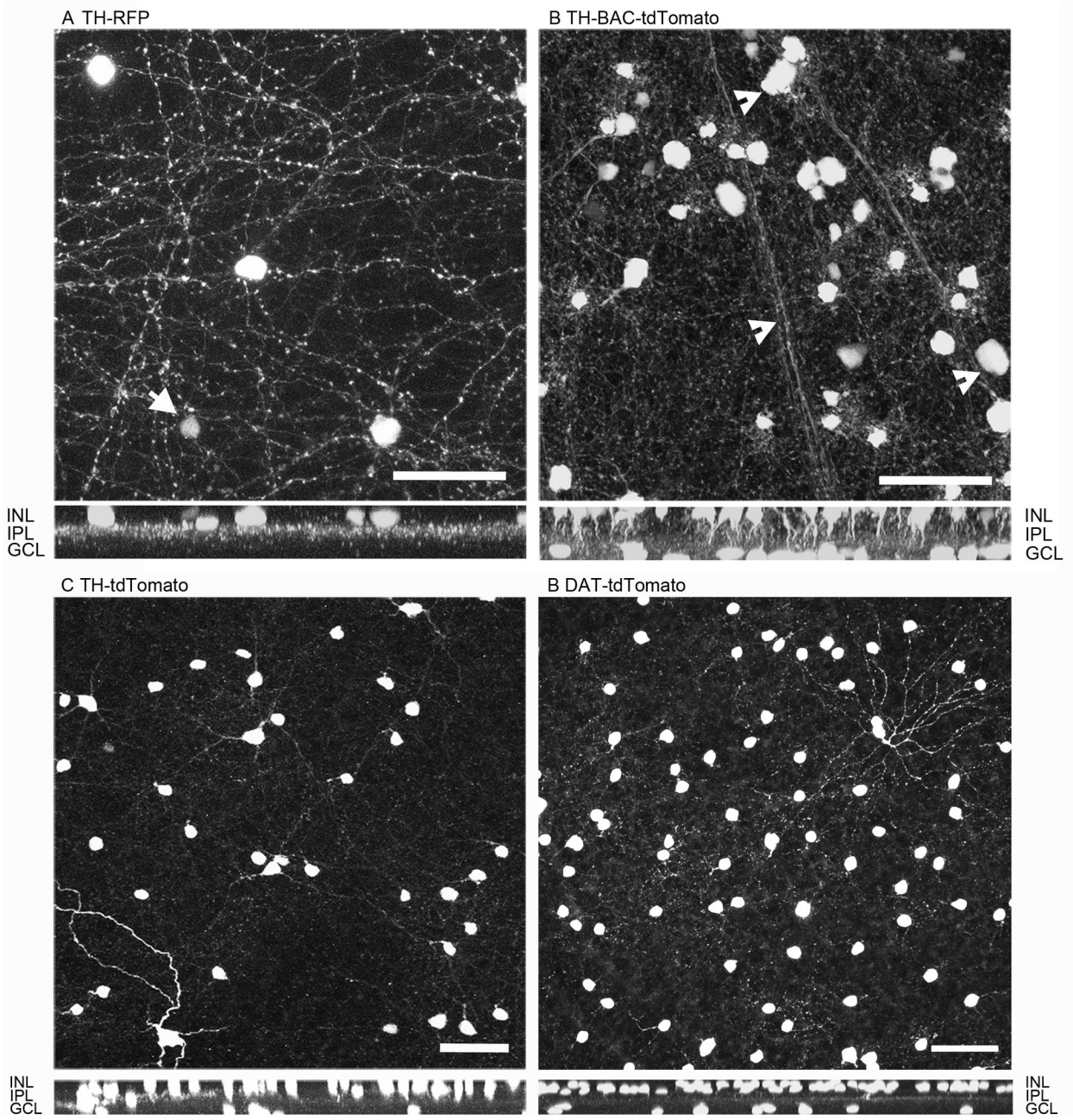

Figure 2. Reporter expression in whole-mounted retinas of the transgenic lines

Reporter expression in whole-mounted retinas was in soma and processes of cells that were distributed throughout the entire retina. **(A)** RFP expression in amacrine cells bodies in the INL and their processes in strata 1 and 2/3 of the IPL. Lower levels of RFP were in smaller soma (arrow). **(B)** tdTomato expression in the TH-BAC-tdTomato line showed extensive labeling of narrow-field amacrine cells, medium-sized amacrine cells, and putative ganglion cells and their axons (arrowheads). **(C)** tdTomato expression in the TH promoter was in cell somata primarily localized in the INL and a few in the GCL. **(D)** tdTomato expression in the DAT-tdTomato line showed extensive labeling of medium-sized amacrine cells. tdTomato

expression under the DAT promoter was in cell somata primarily localized in the INL and a few in the GCL. Bottom panels are the z-plane rotation of the whole mount image. Scale bar: 50 μm.

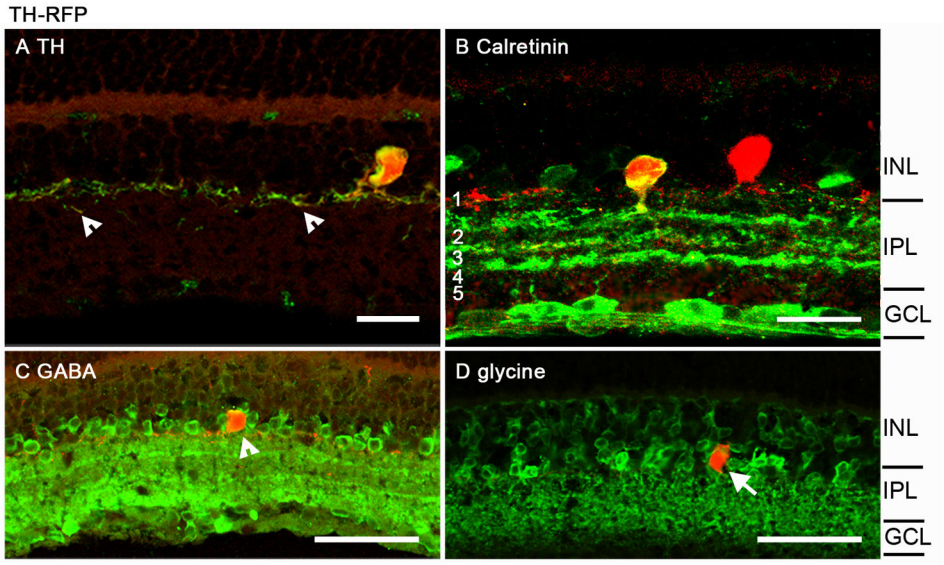

Figure 3. RFP fluorescence compared to TH, calretinin, GABA, and glycine immunoreactivity

Co-localization of TH, calretinin, and GABA immunoreactivity with RFP fluorescence showed the TH-RFP line contained labeled type 1 and 2 DA amacrine cells. **(A)** Large soma sized RFP fluorescent cell (type 1 DA amacrine cells) was co-localized with TH immunoreactivity. Arrowhead: TH immunoreactivity was stronger in fine caliber processes compared to RFP fluorescence. **(B)** Calretinin immunoreactivity was not co-localized with large soma-sized RFP fluorescent cells, but did co-localize with small soma-sized RFP fluorescent cells. RFP labeled processes were in strata 1, 2/3, and weakly in 3. **(C)** All RFP expressing amacrine cells contained GABA immunoreactivity. Arrowhead showed co-localization. **(D)** RFP expressing cells did not contain glycine immunoreactivity. Arrow indicates lack of co-localization between RFP fluorescence and glycine immunoreactivity. Scale bar: 20 μm.

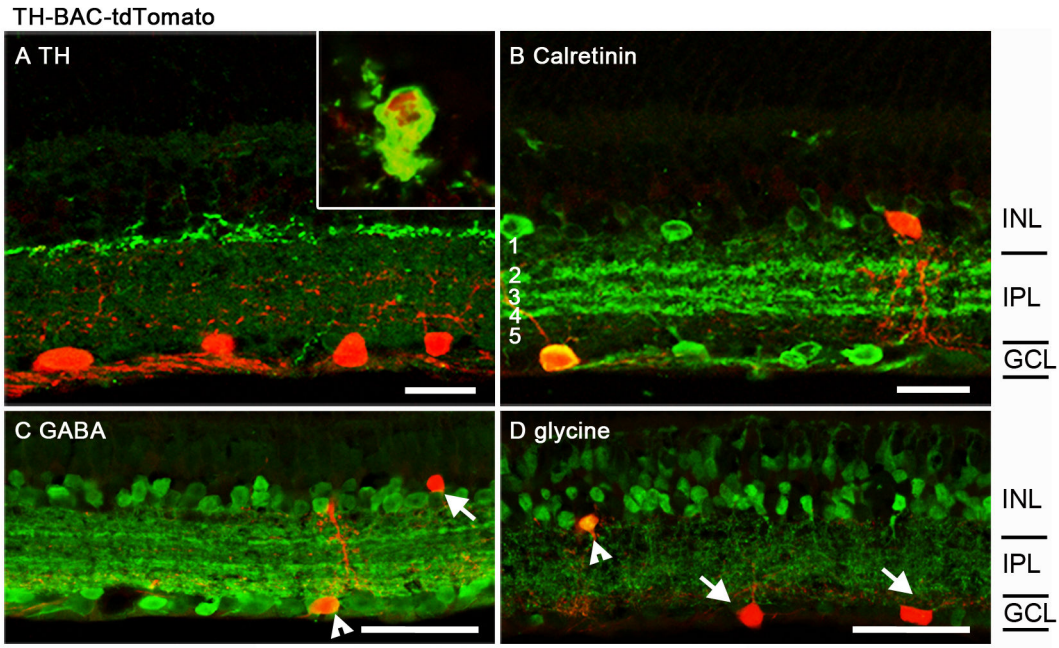

Figure 4. Expression of tdTomato fluorescence and TH, calretinin, GABA, and glycine immunoreactivity in vertical sections of the TH-BAC-tdTomato retinas

(A) TH-BAC-tdTomato cells rarely co-localized with TH immunoreactive amacrine cells. Inset showed a rare case of co-labeling of a cell with tdTomato fluorescence and TH immunoreactivity. **(B)** A subset of TH-BAC-tdTomato expressing cells co-localized with calretinin immunoreactivity in the GCL. **(C)** TH-BAC-tdTomato expression is in some GABA immunoreactive cells. **(D)** There is tdTomato expression in some glycine immunoreactive cells. Arrowheads indicate co-localization. Arrows highlight cells that did not co-localize. Scale bar: 20 μm.

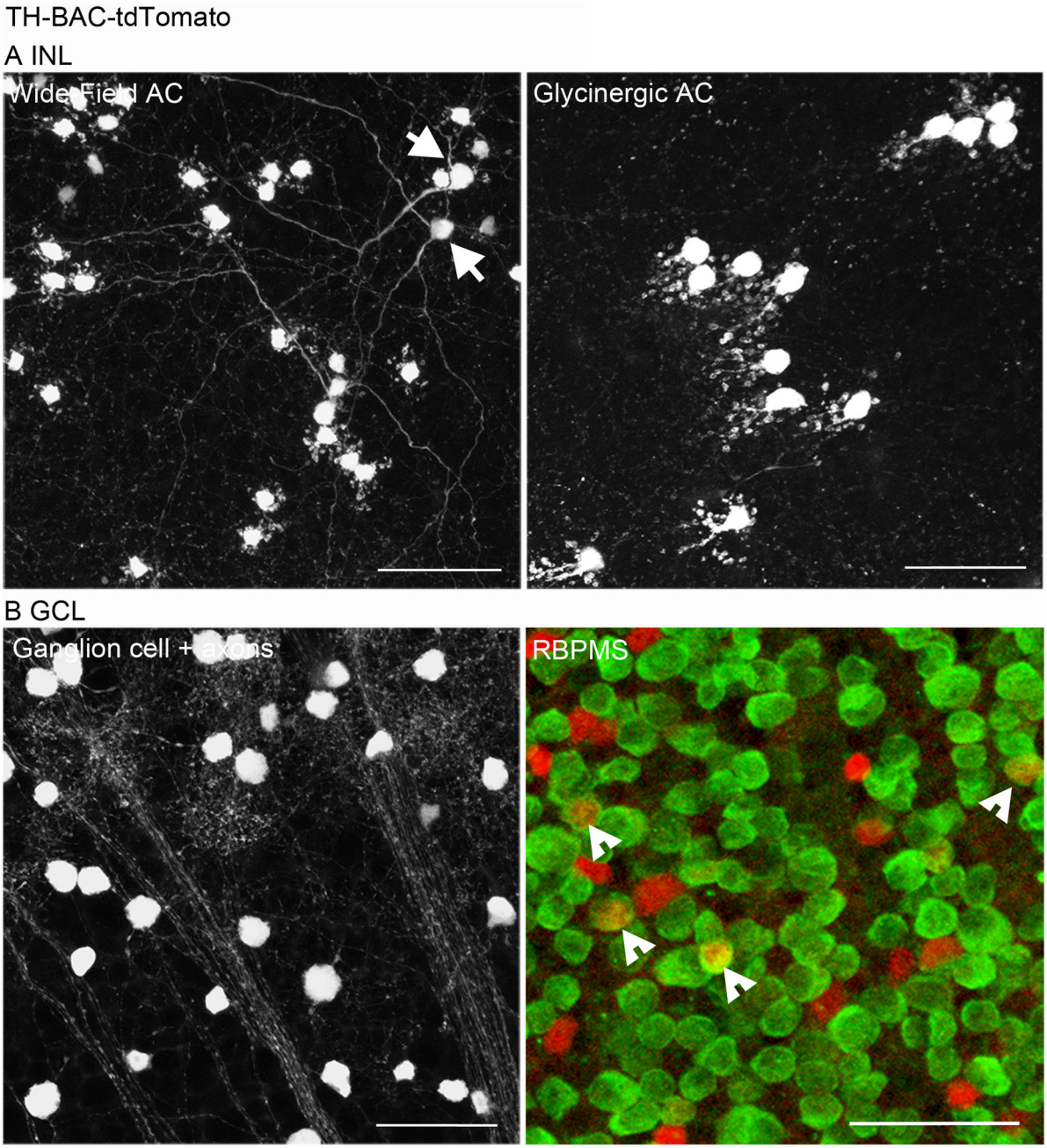

Figure 5. Characterization of TH-BAC-tdTomato whole-mounted retinas reveal several distinct types of amacrine cells

Several amacrine cell types are labeled in the TH-BAC-tdTomato line. **(A)** In the INL there were infrequently occurring wide-field amacrine cells that arborized in the OFF sublamina (left panel, arrows). They had polyaxonal properties, and their processes extended more than 200 μm laterally across the retina. Also in the INL were clusters of glycine immunoreactive amacrine cells. Defined by a narrow-field morphology, these cells were AII amacrine cells (right panel). **(B)** In the GCL tdTomato expression was in displaced amacrine cells, and ganglion cells and their axons (left panel). Arrowheads point to cells co-localized with

RBPMS immunoreactivity, a retinal ganglion cell marker, indicating the presence of tdTomato fluorescent ganglion cells (right panel). Scale bar: 50 μm.

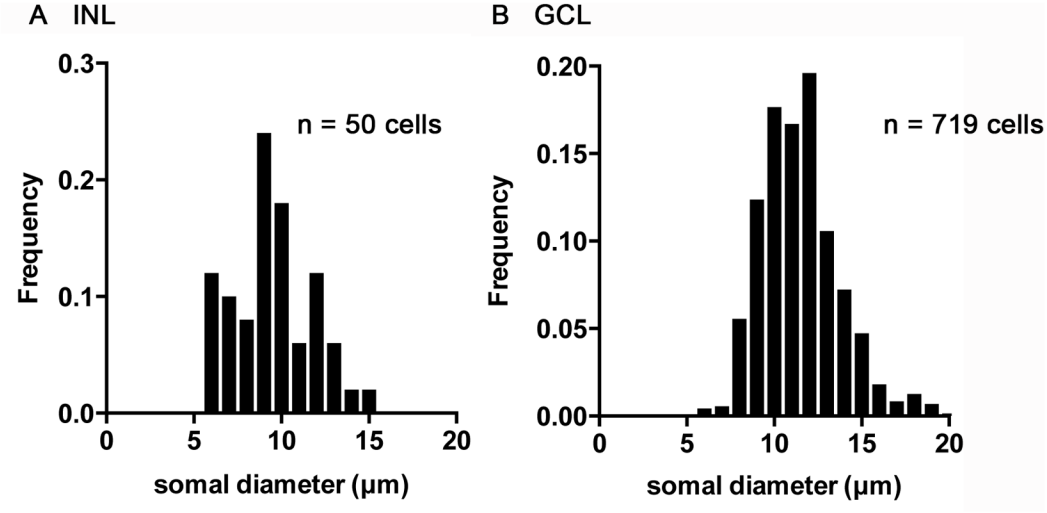

Figure 6. Distribution of co-localized RBPMS immunoreactive cells in TH-BAC-tdTomato retinas

(A) Frequency of co-localized RBPMS somal diameters in the INL. The average somal diameter in the INL was 10.02 ± 2.25 µm (n=50 cells). **(B)** Frequency of somal diameters of RBPMS co-immunoreactive cells in the GCL. The average somal diameter in the GCL was 10.98 ± 2.24 µm (n=719 cells).

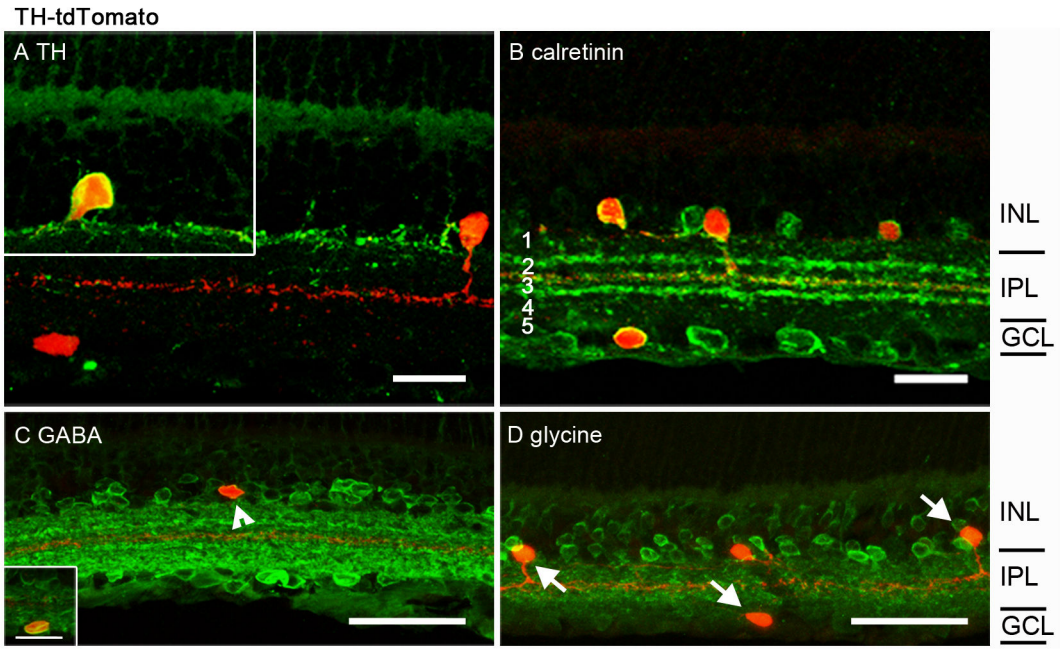

Figure 7. Expression of tdTomato fluorescence and TH, calretinin, GABA, and glycine immunoreactivity in vertical sections of TH-tdTomato retinas

(A) Most tdTomato fluorescent amacrine cells in the INL did not contain TH immunoreactivity. However, there were some amacrine cells in the INL (inset) that co-labeled with TH immunoreactivity. **(B)** Many cells labeled in the TH-tdTomato line co-expressed calretinin immunoreactivity. These cells were in the INL and GCL, and their processes corresponded with strata 1, 2/3, and 4. **(C)** TH-tdTomato expressing cells in transverse sections was primarily GABA immunoreactive, in both the INL (arrowhead) and GCL (inset). **(D)** In vertical sections, tdTomato fluorescence did not co-localize with glycine immunoreactivity (arrows). Scale bar: 20 μm.

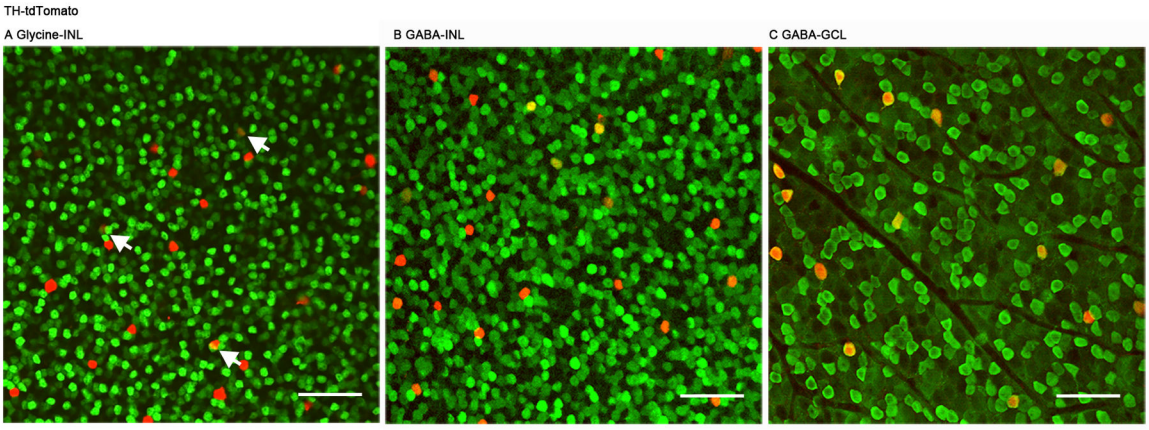

Figure 8. TH-tdTomato expression is limited to amacrine cells

In whole-mount TH-tdTomato retinas, tdTomato fluorescence was in GABA immunoreactive amacrine cells and very few glycine immunoreactive amacrine cells. **(A)** Arrows point to the few tdTomato-expressing cells that co-labeled with glycine immunoreactivity in the INL. (**B)** Most GABA immunoreactivity robustly co-localized with tdTomato expression in the INL. Some tdTomato expressing cells had low levels of GABA immunoreactivity. **(C)** All tdTomato expression in cells in the GCL co-labeled with GABA immunoreactivity. Scale bar: 50 μm

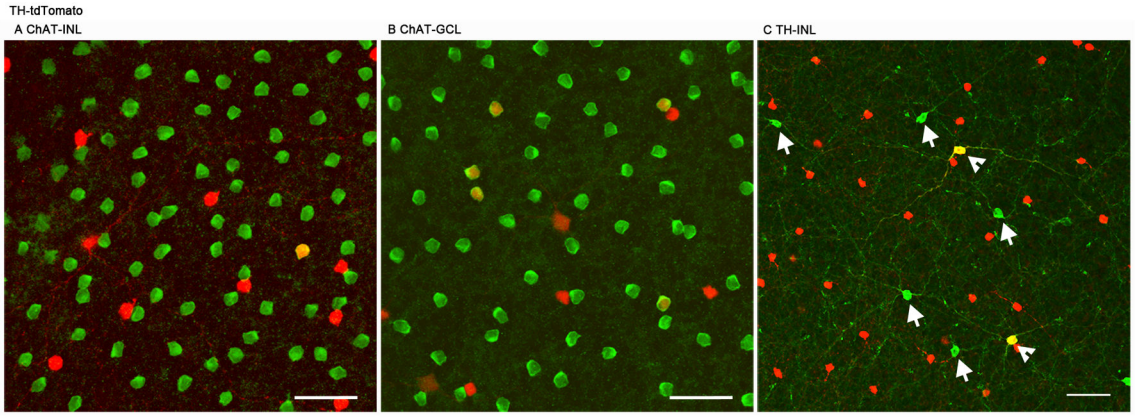

Figure 9. tdTomato fluorescence is in some starburst and type 1 DA amacrine cells in TH-tdTomato retinas

tdTomato fluorescence in the TH-tdTomato line was in a subset of starburst and type 1 DA amacrine cells. **(A)** ChAT immunoreactivity co-localized with a few tdTomato expressing cells in the INL. **(B)** ChAT immunoreactivity was in a subset of tdTomato expressing cells in the GCL. **(C)** TH immunoreactivity co-labeled with some tdTomato expressing cells in the INL (arrowheads), but tdTomato expression was not in all type 1 DA amacrine cells, as indicated by TH immunoreactive cells that lack tdTomato fluorescence (arrows). Scale bar: 50 μm.

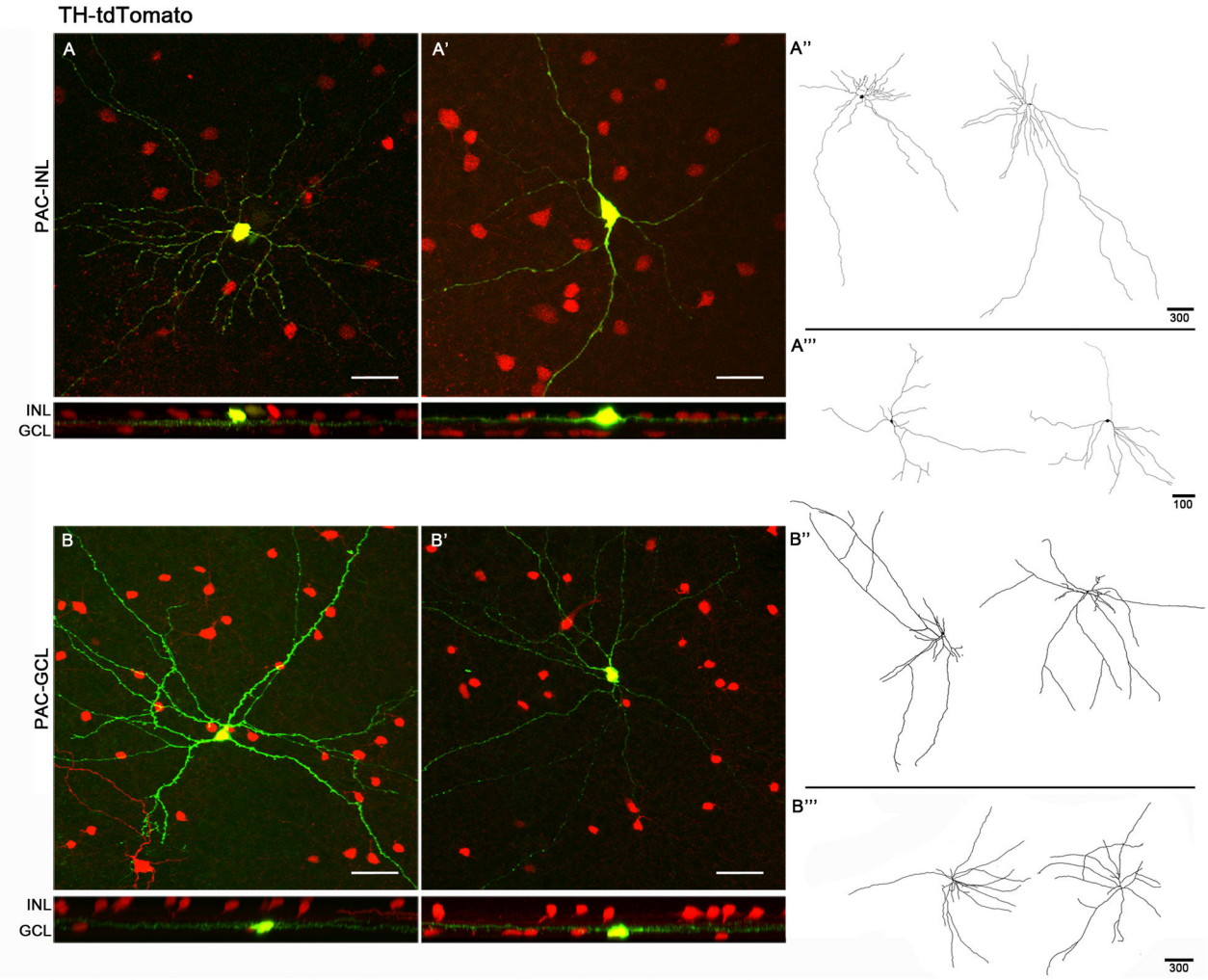

Figure 10. Intracellular injections of Neurobiotin reveals multiple populations of polyaxonal wide-field amacrine cells

tdTomato fluorescence in the TH-tdTomato line labeled different morphological types of polyaxonal wide-field amacrine cells. **(A)** An example of a polyaxonal amacrine cell in the INL with radial and varicose processes that arborized in strata 2 and 3 of the IPL. **(A′)** Intracellular fill of a type 1 DA amacrine cell and its processes were in stratum 1 of the IPL. **(A″)** Cellular reconstruction of a wide-field polyaxonal amacrine cell. **(A‴)** Cellular reconstruction of a type 1 DA amacrine cells in the INL. **(B)** Neurobiotin intracellular injection of a polyaxonal amacrine in the GCL. Processes showed many dendritic spines in stratum 5 of the IPL. **(B′)** An example of a polyaxonal amacrine in the GCL that had varicose processes. **(B″)** Cellular reconstruction of polyaxonal amacrine cell in **B**, which was defined by an asymmetrical dendritic arborization. **(B‴)** Cellular reconstruction of polyaxonal amacrine cell in B′, which was an example of a polyaxonal amacrine cell with varicose and radial dendritic arborizations. Scale bar: A, A′, B, and B′ = 50 μm, A″ = 300 μm, A‴ = 100 μm, B″ and B‴ = 300 μm

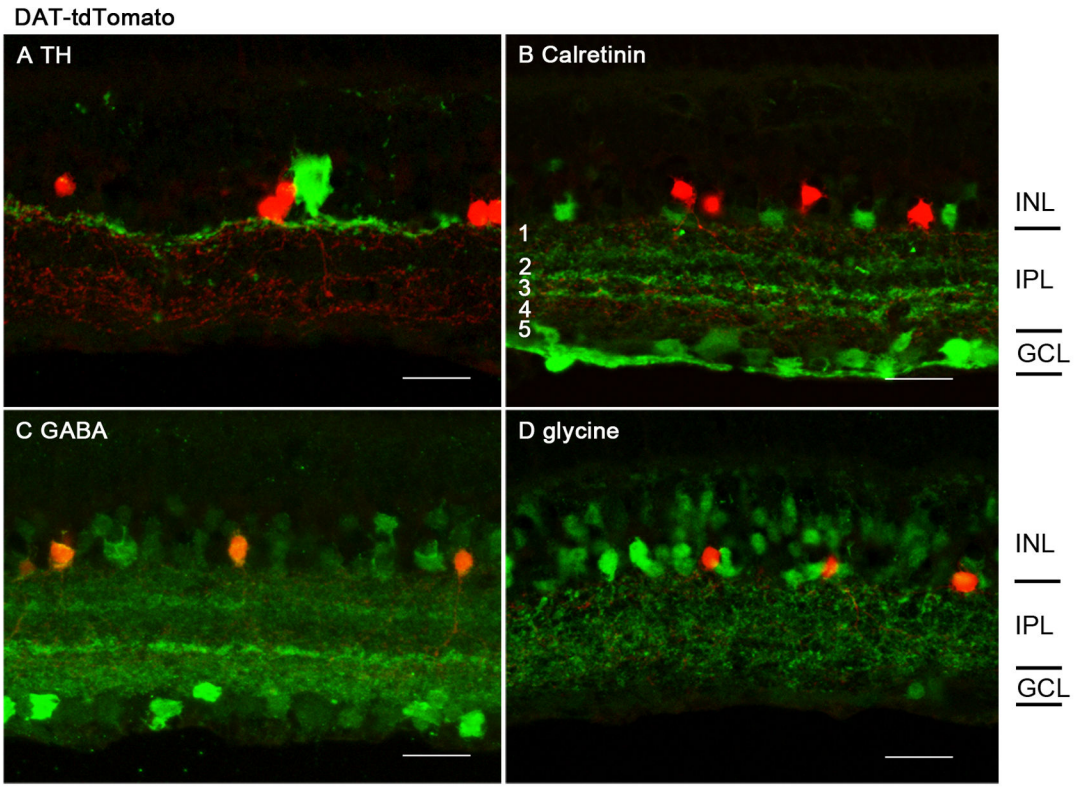

Figure 11. Expression of tdTomato fluorescence compared to TH, calretinin, GABA, and glycine immunoreactivity in vertical sections of DAT-tdTomato retinas

(A) tdTomato fluorescence did not co-localize with TH immunoreactivity. **(B)** tdTomato expression in the DAT-tdTomato line did not co-localize with calretinin immunoreactivity. tdTomato processes were distributed between the calretinin immunoreactive plexuses. The tdTomato processes were in strata 1, 3, 4, and 5. **(C)** All tdTomato fluorescent cells expressed GABA immunoreactivity, **(D)** but they were not glycine immunoreactive. Scale bar: 20 μm.

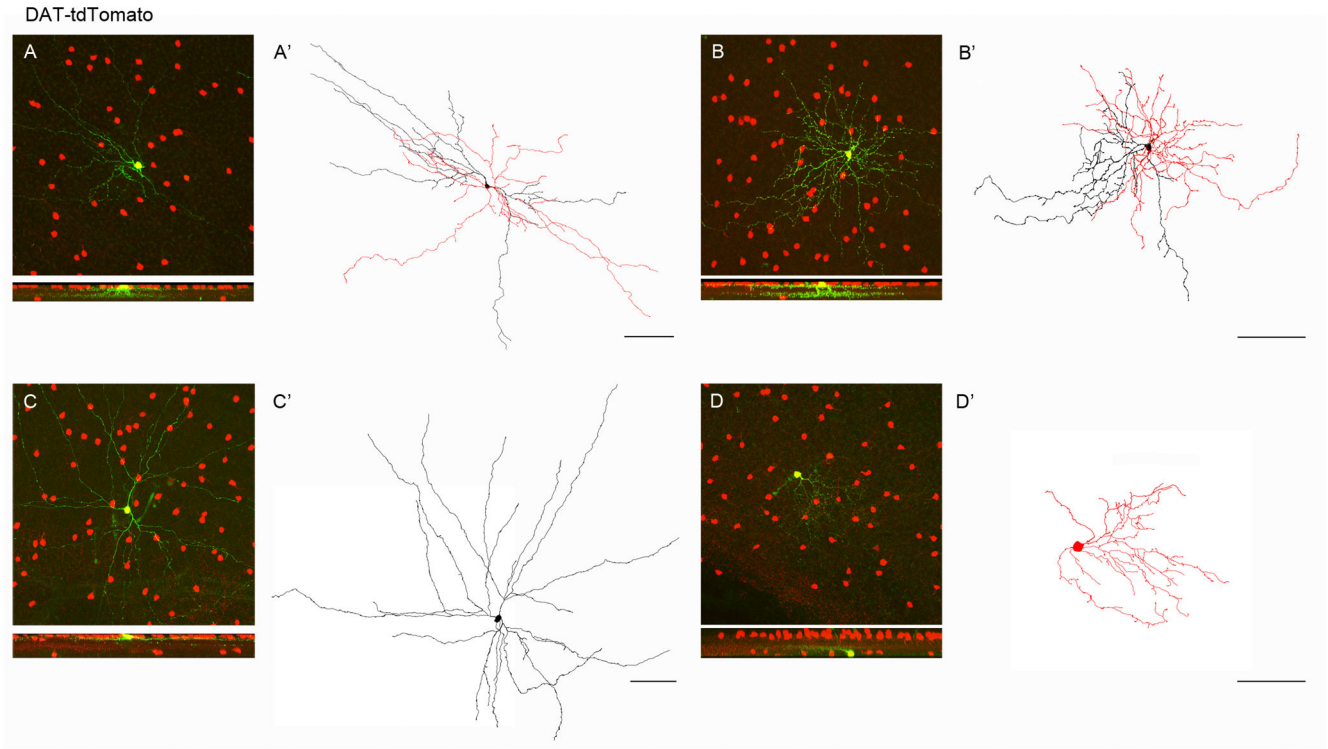

Figure 12. Neurobiotin intracellular injections of DAT-tdTomato fluorescent cells show multiple populations of bistratified and monostratified amacrine cells

DAT-tdTomato expressing cells consisted of multiple populations of amacrine cells. **(A)** An example of a wide-field bistratified amacrine cell in the INL with symmetrical and varicose processes that arborized in strata 1, 4 and 5 of the IPL. **(A′)** Cellular reconstruction of a wide-field bistratified amacrine cell. It had long processes in the OFF sublamina (black) and ON sublamina (red), and extended over 500 μm in diameter. **(B)** Neurobiotin intracellular injection of a medium-field bistratified amacrine cell in the INL. Processes in strata 1, 3, 4, and 5 of the IPL. **(B′)** Cellular reconstruction of medium-field bistratified amacrine cell in **B**, which was defined by radial dendritic arborizations. **(C)** Neurobiotin intracellular injection of a wide-field amacrine in the INL. There were multiple processes that arborized in stratum 1 of the IPL. **(C′)** Cellular reconstruction of the wide-field amacrine cell in **C**, which was defined by long and radial dendritic arborizations. **(D)** Neurobiotin intracellular injection of a displaced amacrine in the GCL. There were multiple processes that arborized in stratum 4 of the IPL. **(D′)** Cellular reconstruction of the displaced amacrine cell in D. Scale bar: 100 μm

Table 1

List of primary antibodies

Antibody	Host	Immunogen	Source	Dilution
calretinin	mouse	Recombinant human calretinin-22k	Swant, Bellinzona, Switzerland; Lot no 010399 clone 6B3	1:2000
ChAT	goat	human placental enzyme	Millipore, Billerica, MA, USA; AB144P	1:250
GABA	rabbit	GABA conjugated with bovine serum albumin (GABA- BSA)	Sigma-Aldrich, St Louis, MO, USA; A2052	1:2000
glycine	rat	Glycine conjugated to paraformaldehyde and carrier protein thyroglobulin	ImmunoSolution, Everton Park QLD, Australia; IG1002	1:3000
RBPMS	guinea pig	$RBPMS_{4-24}$ with N- terminal cys; GGKAEKENTPSEA NLQEEEVRC-KLH conjugate	Rodriguez et al. 2014; GP15029-3, GP15029- FRB15027-3	1:20000
tyrosine hydroxylase	mouse	Purified tyrosine hydroxylase (EC 1.14.16.2) from a rat pheochromocytoma	Millipore, Billerica, MA, USA; MAB5280 clone 2/40/15	1:2000

Table 2

Summary of density and somal size

transgenic animal line	# of transgenic cells per mm^2 (mean ± SD)	somal size (μm) (mean ± SD)	
TH-RFP	type 1: 37 ± 17 type 2: 181 ± 54	12.43 ± 2.33 9.89 ± 1.24	
		INL:	GCL:
TH-BAC-tdTomato	1793 ± 731	6.48 ± 1.04[a] 9.10 ± 0.57[b] (0.92%)	6.86 ± 1.06[c] 10.54 ± 1.53[d] (30.51%)
		INL:	GCL:
TH-tdTomato	189 ± 37	6.76 ± 0.99[a] 10.10 ± 1.49[b] (10.84%)	7.25 ± 1.02[e] 10.34 ± 1.40[f] (10.22%)
		INL:	GCL:
DAT-tdTomato	646 ± 160	8.97 ± 1.06	9.08 ± 1.61

[a] glycine-immunoreactive amacrine cells with small somal sizes

[b] GABA-immunoreactive amacrine cells with large somal sizes (0.92% or 10.84% of transgenic cells in INL)

[c] displaced amacrine cells with small somal sizes

[d] displaced amacrine and ganglion cells with large somal sizes (30.51% of transgenic cells in GCL)

[e] displaced amacrine cells with small somal sizes

[f] displaced amacrine cells with large somal sizes (10.22% of transgenic cells in GCL)

Table 3

Summary of immunohistochemical labeling

transgenic animal line		immunoreactivityM	% colocalized	
TH-RFP	type 1	anti-TH	100	
		anti-GABA	100	
	type 2	anti-TH	0	
		anti-GABA	100	
TH-BAC-tdTomato		anti-TH	0.32 ± 0.06	
			INL:	GCL:
		anti-GABA	8.51 ± 0.40	74 ± 1.7
			INL:	GCL:
		anti-glycine	85.11 ± 1.51	0
		anti-calretinin	9.06 ± 1.23	
			INL:	GCL:
		anti-RBPMS	0.46 ± 1.41	24.21 ± 12.17
TH-tdTomato		anti-TH	5.95 ± 1.53	
		anti-GABA	89.11 ± 1.9	
		anti-glycine	1.50 ± 0.03	
		anti-calretinin	81.08 ± 1.35	
		anti-ChAT	6.10 ± 1.99	
DAT-tdTomato		anti-TH	0	
		anti-GABA	100	
		anti-calretinin	0	